Editor-in-Chief
Dr. Kouroush Jenab

INTERNATIONAL JOURNAL OF
ENGINEERING (IJE)

ISSN : 1985-2312

Volume 7 • Issue 1 • April 2013
Publication Frequency: 6 Issues / Year

CSC PUBLISHERS
http://www.cscjournals.org

INTERNATIONAL JOURNAL OF ENGINEERING (IJE)

VOLUME 7, ISSUE 1, 2013

EDITED BY
DR. NABEEL TAHIR

ISSN (Online): 1985-2312

International Journal of Engineering is published both in traditional paper form and in Internet. This journal is published at the website http://www.cscjournals.org, maintained by Computer Science Journals (CSC Journals), Malaysia.

IJE Journal is a part of CSC Publishers

Computer Science Journals

http://www.cscjournals.org

INTERNATIONAL JOURNAL OF ENGINEERING (IJE)

Book: Volume 7, Issue 1, February 2013
Publishing Date: 30-04-2013
ISSN (Online): 1985-2312

IJE Journal is a part of CSC Publishers
http://www.cscjournals.org

Published in Malaysia

Typesetting: Camera-ready by author, data conversation by CSC Publishing Services – CSC Journals, Malaysia

CSC Publishers, 2013

EDITORIAL PREFACE

This is the *First* Issue of Volume *Seven* for International Journal of Engineering (IJE). The Journal is published bi-monthly, with papers being peer reviewed to high international standards. The International Journal of Engineering is not limited to a specific aspect of engineering but it is devoted to the publication of high quality papers on all division of engineering in general. IJE intends to disseminate knowledge in the various disciplines of the engineering field from theoretical, practical and analytical research to physical implications and theoretical or quantitative discussion intended for academic and industrial progress. In order to position IJE as one of the good journal on engineering sciences, a group of highly valuable scholars are serving on the editorial board. The International Editorial Board ensures that significant developments in engineering from around the world are reflected in the Journal. Some important topics covers by journal are nuclear engineering, mechanical engineering, computer engineering, electrical engineering, civil & structural engineering etc.

The initial efforts helped to shape the editorial policy and to sharpen the focus of the journal. Started with volume 7, 2013, IJE appears with more focused issues. Besides normal publications, IJE intend to organized special issues on more focused topics. Each special issue will have a designated editor (editors) – either member of the editorial board or another recognized specialist in the respective field.

The coverage of the journal includes all new theoretical and experimental findings in the fields of engineering which enhance the knowledge of scientist, industrials, researchers and all those persons who are coupled with engineering field. IJE objective is to publish articles that are not only technically proficient but also contains information and ideas of fresh interest for International readership. IJE aims to handle submissions courteously and promptly. IJE objectives are to promote and extend the use of all methods in the principal disciplines of Engineering.

IJE editors understand that how much it is important for authors and researchers to have their work published with a minimum delay after submission of their papers. They also strongly believe that the direct communication between the editors and authors are important for the welfare, quality and wellbeing of the Journal and its readers. Therefore, all activities from paper submission to paper publication are controlled through electronic systems that include electronic submission, editorial panel and review system that ensures rapid decision with least delays in the publication processes.

To build its international reputation, we are disseminating the publication information through Google Books, Google Scholar, Directory of Open Access Journals (DOAJ), Open J Gate, ScientificCommons, Docstoc and many more. Our International Editors are working on establishing ISI listing and a good impact factor for IJE. We would like to remind you that the success of our journal depends directly on the number of quality articles submitted for review. Accordingly, we would like to request your participation by submitting quality manuscripts for review and encouraging your colleagues to submit quality manuscripts for review. One of the great benefits we can provide to our prospective authors is the mentoring nature of our review process. IJE provides authors with high quality, helpful reviews that are shaped to assist authors in improving their manuscripts.

Editorial Board Members
International Journal of Engineering (IJE)

TABLE OF CONTENTS

Volume 7, Issue 1, April 2013

Pages

Area Efficient and Reduced Pin Count Multipliers

Omar Nibouche *o.nibouche@tu.edu.sa*
College of Computers and Information Technology
Taif University
POB 888 Taif 21964, KSA

Abstract

Fully serial multipliers can play an important role in the implementation of DSP algorithms in resource-limited chips such as FPGAs; offering area efficient architectures with a reduced pin count and moderate throughput rates. In this paper two structures that implement the fully serial multiplication operation are presented. One significant aspect of the new designs is that they are systolic and require near communication links only. They are superior in speed and area usage to similar architectures in the literature. The paper also present a new fully serial multiplier optimized for area-time^2 efficiency with better performance than available architectures in the open literature.

Keywords: Reduced Pin Count, Serial Multiplication, Area-Time^2.

1. INTRODUCTION

There is a crucial advantage offered by bit-serial processors over their parallel counterpart, which lies in the very efficient use of chip area. They are particularly suitable for applications that require slow to moderate speeds and in batch mode applications. By contrast, bit-parallel processors are useful for fast speed systems, but at the expense of larger a area usage and thus they are more expensive [1-2].

Traditional bit serial multiplier structures suffer from an inefficient generation of partial products, which leads to hardware overuse and slow speed systems. In this paper, two structures for bit serial multiplication are presented. The first structure, called *structure I*, is the first fully serial multiplier reported in the literature with comparable performance - in terms of speed- to existing serial-parallel multipliers. The second structure, termed *structure II*, requires an extra multiplexer in the clock path; thus making it slower, but has the merit of reducing the latency of the multiplier.

The remainder of the paper is organised as follows: in section 2, the previous work in the literature is reviewed, while section 3 describes the new structures for fully serial multiplication. Section 4 is concerned with an optimisation of the multiplier of *Structure I* in terms of area-time^2 efficiency. A comparison of performance is shown in section 5 and conclusions are given in section 6.

2. BIT SERIAL MULTIPLIERS: A REVIEW

One of the early bit serial multipliers was proposed by [3]. It generates the partial products in a recursive fashion. Consider the multiplication of two n-bit positive numbers *A* and *B* as follows:

$$A = \sum_{i=0}^{i=n-1} a_i 2^i \tag{1}$$

and

$$B = \sum_{i=0}^{i=n-1} b_i 2^i \tag{2}$$

Let P_i represents the partial product computed after the i[th] bit is fed [3]. P_i is given by:

$$P_i = P_{i-1} + 2^i (a_i B_{i-1} + b_i A_{i-1}) + 2^{2i} a_i b_i \quad (3)$$

where A_i and B_i represent the value of the operands A and B, respectively, and by considering only bits from the Least Significant Bit (LSB) to the i[th] bit, that is,

$$A_i = A \bmod 2^{i+1} \quad (4)$$

and

$$B_i = B \bmod 2^{i+1} \quad (5)$$

with the initial values $P_{-1} = A_{-1} = B_{-1} = 0$.

The generation of the partial product, using equation (3), and their assignment to the multiplier cells is shown in Table 1 below:

Cycle	P	Cell 1	Cell 2	Cell 3	Cell 4
1	P_0	a_0b_0			
2	P_1	$a_0b_1+a_1b_0$	a_1b_1		
3	P_2	$a_0b_2+a_2b_0$	$a_1b_2+a_2b_1$	a_2b_2	
4	P_3	$a_0b_3+a_3b_3$	$a_1b_3+a_3b_1$	$a_2b_3+a_3b_2$	a_3b_3
5	P_4	↙	↙	↙	↙
6	P_5	↙	↙	↙	
7	P_6	↙	↙		
8	P_7	↙			

TABLE 1: Multiplication Scheme of [3].

From the above table, each cell generates two new bit-products every cycle. To cope with this constraint, The Basic Cell (BC) of the multiplier proposed by [3] is built around a 5 to 3 counter. The counter is capable of accumulating five inputs of the same weight to a sum-bit (S_{out}) of the same weight as the inputs, i.e.2^0, 1[st] carry-bit (C^1_{out}) of a weight of 2^1 and 2[nd] carry-bit (C^2_{out}) of a weight of 2^2. In particular, the sum-bit is calculated through a tree of EXOR gate to reduce the propagation delay within the cell. The BC of the multiplier is shown in Figure 1. The multiplier uses n identical cells to perform the multiplication of two n-bit numbers in $2n$ cycles, as it can be seen in Figure 2.

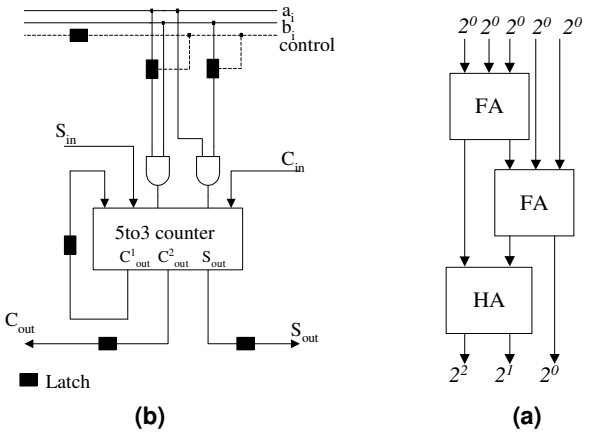

FIGURE 1 (a): 5 to 3 Counter Made of Two FAs and One HA **(b).** The BC of [3].

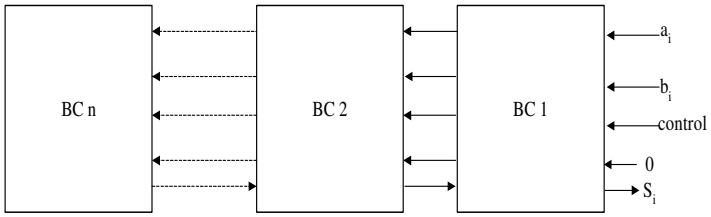

FIGURE 2: The n-bit Multiplier by [3].

In [4], modifications were carried out on the multiplication scheme of Table 1 to make a more efficient use of the hardware. In fact, the multiplier proposed by [4] uses only half the number of cells required by [3]. To achieve this, the partial products generated by the last *n/2* cells in [3] were reallocated to the first *n/2* cells and rescheduled at cycle *n+1*. In this way, a full utilisation of cells *1* to *n/2* can be achieved, as it can be shown in Table 2.

Cycle	P	Cell 1	Cell 2
1	P_0	a_0b_0	
2	P_1	$a_0b_1+a_1b_0$	a_1b_1
3	P_2	$a_0b_2+a_2b_0$	$a_1b_2+a_2b_1$
4	P_3	$a_0b_3+a_3b_3$	$a_1b_3+a_3b_1$
5	P_4	a_2b_2	a_3b_3
6	P_5	$a_2b_3+a_3b_2$	↙
7	P_6	↙	
8	P_7	↙	

TABLE 2: Multiplication Scheme by [4].

The multiplier was modified using little extra hardware: two *n/2* shift registers are used to store the *n/2* most significant bits of the data words *A* and *B* and *n/2* multiplexers. The BC of the modified multiplier d is shown in Figure 3. The multiplier structure as proposed by [4] is shown in Figure 4. This architecture has reduced the number of 5 to 3 counters by 50%, as well as reducing the number of latches by 33%. The clock path equals the delay of a multiplexer, a gated counter and a latch.

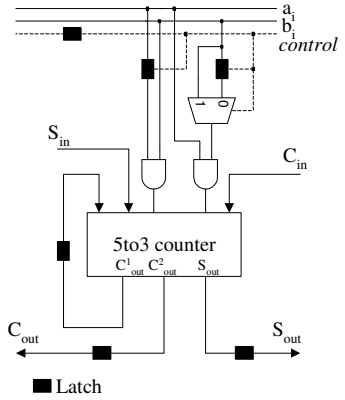

FIGURE 3: The BC of [4].

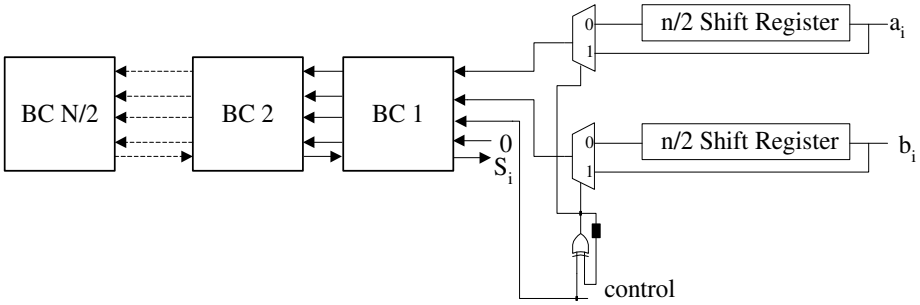

FIGURE 4: The n-bit Multiplier by [4].

3. THE NEW FULLY SERIAL MULTIPLIERS

Although about 50% of the area used in [3] has been saved by [4], the throughput rate has not been increased. On the contrary, it has decreased as a multiplexer was added to the structure making the clock period of the multiplier in [4] equivalent to the delay of a multiplexer, an AND gate, a 5 to 3 counter and a latch. To remedy this problem, two new structures are proposed.

3.1. *Structure I*

In order to reduce the clock path as described above, the multiplication algorithm has been modified. It generates the bit-products associated with cells *2* to *n* at the $(n+1)^{th}$ cycle. The scheduling of the tasks of the first cell is kept unchanged, but the latency of the multiplier is increased to *n* cycles. The multiplication scheme is shown in Table 3 for 4-bit operands. The multiplication operation can be divided into two parts, which can easily be done by rewriting the product of the two numbers, *A* and *B*, in the following way:

$$A * B = a_0 B + \sum_{i=1}^{i=n-1} \sum_{j=0}^{j=n-1} a_i b_j 2^{i+j} \quad (6)$$

To keep working under the constraints of sending one bit of each operand at a time, the term a_0B in equation (6) is generated by the first cell of the multiplier during the first n cycles. At this stage, the other cells only propagate the partial products already generated by the first cell. At the $(n+1)^{th}$ cycle, all the operand bits have been fed and the term $\sum_{i=1}^{i=n-1}\sum_{j=0}^{j=n-1} a_i b_j 2^{i+j}$ can be generated during the last n cycles. The clock period is equivalent to the delay of a FA, an AND gate and a latch, as shown in Figure 5. Therefore, *Structure I* achieves similar speed performances when compared with serial-parallel multipliers.

3.2. *Structure II*

The 5 to 3 counters have been widely used in the literature [3-6]. Basically, such a counter reduces 5 bits of the same weight to three bits: a result-bit of the same weight as the inputs (a weight of 2^0), a carry-bit, which has a weight of 2^1, and a far carry-bit that has a weight of 2^2. It is clear that while the sum of the inputs is up to 5, the sum of the outputs is up to 6, and as such, two representations of the outputs are excluded. Therefore, it is clearly more appropriate to reduce the 5 inputs to 3 outputs: a result-bit of the same weight as the inputs, and 2 carry-bits of twice the weight of the result-bit. For this purpose, a new cell has been developed by using two FAs as shown in Figure 6. The first FA is used to accumulate two bit products with a carry feedback. The second FA is used to generate a result-bit from the result of the first FA, the result-bit from the adjacent cell and a carry feedback. The two carry-bits generated by the new cell are fed back and accumulated with the bit-products of the next cycle. The sum-bit of the first FA is registered, and thus making the clock period equivalent to the delay of a multiplexer, an AND gate, a FA and a latch. The multiplier structure implements directly the algorithm shown in Table 2. The multiplier requires only $n/2$ cells for the multiplication of two n-bit numbers. It is also modular and needs near communication links only.

TABLE 3: *Structure I* Multiplication Scheme For 4-bit Operands.

Cycle	P	Cell 1	Cell 2	Cell 3	Cell 4
1		a_0b_0			
2		a_0b_1	↘		
3		a_0b_2	↘	↘	
4	P_0	a_0b_3	↘	↘	↘
5	P_1		a_3b_0	a_2b_0	a_1b_0
6	P_2		a_3b_1	a_2b_1	a_1b_1
7	P_3		a_3b_2	a_2b_2	a_1b_2
8	P_4		a_3b_3	a_2b_3	a_1b_3
9	P_5		↘	↘	↘
10	P_6			↘	↘
11	P_7				↘

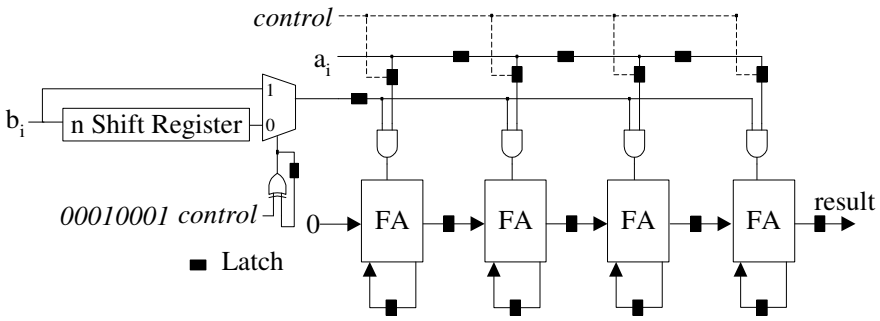

FIGURE 5: *Structure I* bit-bit Serial Multiplier.

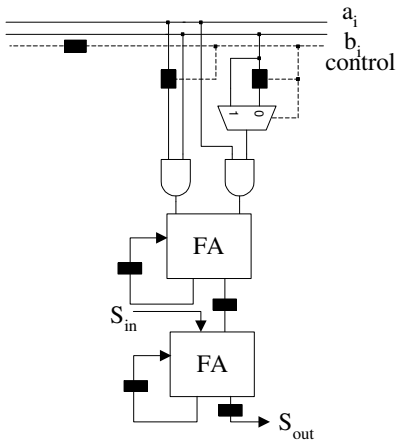

FIGURE 6: The Basic Cell of *Structure II* Fully Serial Multiplier

4. AREA-TIME^2 EFFICIENT BIT-BIT SERIAL MULTIPLIER

In this section, a new multiplier structure, which is capable of multiplexing two multiplication operations into *Structure I* is proposed. This has the merit of doubling the throughput rate at the expense of extra hardware consisting of *2n* multiplexers and *n* latches. By optimizing the multiplier for *area-time*^{2} efficiency, the problem of lost cycles is circumvented. The lost cycles are the cycles needed for carry propagation once the generation of the partial-products is finished.

The best structure in the literature that can multiplex two multiplication operations into the same multiplier was described in [7]. The algorithm presented in [7] is an improvement made on the multiplication scheme of Table 2. Starting from this multiplication scheme, it reassigns and reschedules the partial products generated by the $(n/4+1)^{th}$ cell and above starting at $(n+n/4)^{th}$ cycle to the cells from *1* to *n/4* at the $(n+n/2)^{th}$ cycle, respectively. This has the effect of freeing *n/4* most significant cells at the $(n+n/4)^{th}$ cycle and thereafter. The multiplication scheme adopted by [7] to achieve this operation is shown in Table 5.

Cycle	P	Cell 1	Cell 2
1	P_0	a_0b_0	
2	P_1	$a_0b_1+a_1b_0$	a_1b_1
3	P_2	$a_0b_2+a_2b_0$	$a_1b_2+a_2b_1$
4	P_3	$a_0b_3+a_3b_0$	$a_{13}+a_3b_1$
5	P_4	a_2b_2	↙
6	P_5	$a_2b_3+a_3b_2$	
7	P_6	a_3b_3	↙
8	P_7	↙	

TABLE 5: Multiplication Scheme of [7].

Although the work presented in [7] can be applied to the multiplier of *Structure II*, it is easier to optimize the multiplier of *Structure I* for area-time^2 efficiency. One can clearly observe that the result from the first cell is not accumulated with the bit products of the other cells until the $(n+1)^{th}$ cycle. Therefore, instead of feeding the result of the first cell to its neighbouring cell, it is delayed by *n* cycles using *n* latches before being accumulated with the rest of the partial products, as can be seen in Figure 7. In this way, the first cell is used for *n* cycles to generate the bit-products of the first multiplication operation, then is reinitialised during one cycle before being used to generate the bit-products of the second multiplication operation for a duration of another *n* cycles and so on. The remaining cells operate almost in the same fashion. The key point is that they generate and accumulate the bit products of the first pair of operands only when the first cell has finished producing its bit-products. This operation lasts for *n* cycles before the propagation of the partial results is switched to the multiplexers, which allows the cells to generate and accumulate the bit-product of the second pair of data. Consequently, two multiplication operations can be multiplexed into this multiplier every *2n* cycles. The proposed architecture is depicted in Figure 6.

5. COMPARISON OF PERFORMANCE

A performance comparison of the new proposed architectures with similar structures available in the literature [3,4] in terms of area usage and the speed of the multipliers is presented in Table 6. In terms of speed, the multiplier of *Structure I* has a clock period equivalent to the delay of a FA, an AND gate and a latch, and as such operates at faster speeds. Furthermore, the multiplier of *Structure II* has a clock period of a multiplexer, an AND gate, a FA and a latch which makes it faster than the multiplier described in [3]. In terms of area usage, the improvements introduced in [4] on the multiplier of [3] have resulted in saving half the total number of cells. In terms of FPGA area usage and in the case of n-bit operands, *Structure I* is mapped into *5n/2* slices of a virtex-4 FPGA and *Structure II* uses *2n* slices. The multiplier given in [3] is mapped into *5n* slices while the multiplier described in [4] requires *2n* slices. These results clearly show the advantages of the new structures in terms of both speed and area usage.

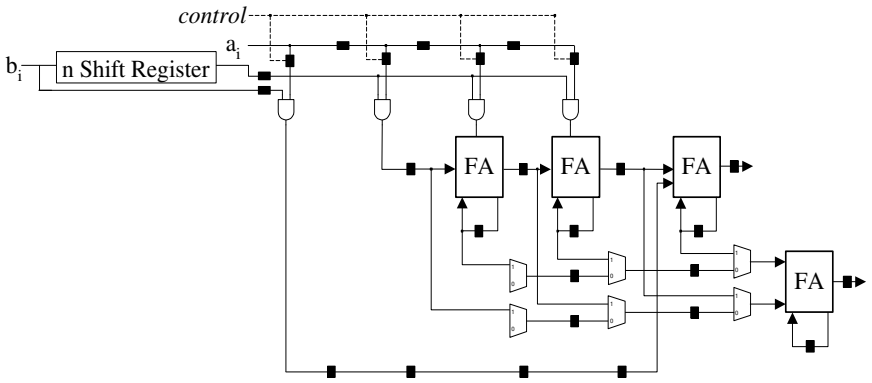

FIGURE 7: The New Area-Time^2 Efficient Multiplier.

	Multiplier in [3]	Multiplier in [4]	*Structure I*	*Structure II*
Basic Cell	counter + 2 AND gates+ multiplexer + 6 latches	Counter + 2 AND gates + 6 latches + multiplexer	FA + AND gate + 4 latches	2 Fas + 2 AND gates + multiplexer + 6 latches
n-bit multiplier area usage	n BCs	n/2 BCs + n + latches	n BCs + n latches	n/2 BCs + n latches
Longest path	AND gate + counter + multiplexer + latch	AND gate + counter + multiplexer + latch	AND gate + FA + latch	AND gate + FA + multiplexer + latch
Latency	1 cycle	1 cycle	n cycles	2 cycles
n-bit multiplier area usage in FPGA Virxtex-4	5n slices	2n slices	5n/2 slices	2n slices

TABLE 6: Performance Comparison.

	Multiplier in [7]	New multiplier
Basic Cell	counter + 2 AND gates+ multiplexer + 6 latches	FA + AND gate + 4 latches
n-bit multiplier area usage	3n/4 BCs + 2n latches ≈63n gates (100%)	n BCs + 4n latches + 2n multiplexers ≈66n gates (104%)
Longest path	AND gate + counter + multiplexer + latch	AND gate + FA + latch

TABLE 8: Performance Comparison of Area-Time^2 Efficient Structures.

Table 8 shows a comparison of performance in terms of hardware usage and speed between the new area-time^2 efficient multiplier and the multiplier described in [7]. An estimation of the area usage for both structures made on the number of gates is also shown. It is assumed that the area of the 5 to 3 counter is equal to that of two FAs and a Half Adder, as shown in Figure 1a, which has the same behavior as the 5 to 3 counter. The area usages of both structures are almost similar, but the BCs and the longest path have not been changed. It is worth pointing out the reason behind the choice of the multiplication scheme of Table 4. One may comment that a *"parallel to serial converter"* added to a bit serial-parallel multiplier transforms it to a fully serial multiplier with identical features to those of *Structure I* multiplier. Had this approach been adopted, once the multiplier is optimised for area-time^2 efficiency, an extra *n* multiplexers would

have been added to the multiplier. These multiplexers are to be added in the path of the data making its clock path equal to the delay of a multiplexer, a gated FA and a latch; making it slower than the multiplier derived from *Structure I.*

6. CONCLUSIONS

In this paper, new structures for reduced pin count multiplication architectures have been presented. These multipliers are systolic and scalable, thus suitable for VLSI implementation. They are both modular and need near communication links only. *Structure I* is the first bit-bit serial multiplier with speed performances similar to existing serial-parallel multipliers. In *Structure II*, the basic cell has been modified to a more appropriate 5 to 3 counter, thus increasing the throughput rate of the multiplier. *Structure I* has been optimised for Area-Time^2 efficiency, which has resulted in doubling the throughput rate.

7. REFERENCES

[1] K.K. Parhi, "VLSI Digital Signal Processing Systems: Design and Implementation", A Wiley-Interscience Publication, 1999.

[2] A. Aggoun, A. Farwan, M.K. Ibrahim and A.S. Ashur, “Radix-2^n Serial-Serial Multipliers”, IEE proc. Circuits, Devices and Systems, vol. 151, issue 6, pp. 503-509, Dec. 2004.

[3] P. Ienne, and M. Viredaz, “A bit-serial multipliers and squarers”, IEEE Trans. Computer, 1994, 43, (12), pp.1445-1450.

[4] A. Aggoun, A.S. Ashur, and M.K. Ibrahim, “Area-Time efficient serial-serial multipliers”, IEEE International Symp. On Circuits and Systems (ISCAS), pp.V-585-588, GENEVA, May 2000.

[5] N. Strader and V. Rhyne, “A canonical bit-sequential multiplier”, IEEE Trans. Computer, 1982, vol. 31, pp. 691-626.

[6] J. Scanlon and W. Fuchs, “'High-performance bit-serial multiplication”, in Proc. IEEE ICCD'86, Rye Brook, NY, Oct. 1986.

[7] A.S. Ashur, “New Efficient Multiplication Structure and their Applications”. Ph.D. thesis, Dept. of Electrical and Electronic Eng., the University of Nottingham, 1996.

Numerical Study of Flow Separation Control by Tangential and Perpendicular Blowing on the NACA 0012 Airfoil

Kianoosh Yousefi *Kianoosh_py@yahoo.com*
Department of Mechanical Engineering
Islamic Azad University, Mashhad Branch
Mashhad, 91735-413, Iran

S. Reza Saleh *s_r_saleh@yahoo.com*
Department of Mechanical Engineering
Islamic Azad University, Mashhad Branch
Mashhad, 91735-413, Iran

Peyman Zahedi *pzahedi96@yahoo.com*
Department of Mechanical Engineering
Islamic Azad University, Mashhad Branch
Mashhad, 91735-413, Iran

Abstract

In this study, tangential and perpendicular steady blowing at the trailing edge of NACA 0012 airfoil is investigated numerically to flow separation control and to study the effects of blowing amplitude and blowing coefficient on airfoil aerodynamic characteristics. Flow was fully turbulent with the Reynolds number of 5×10^5 and the turbulent employed model was the Menter's shear stress model. Blowing on airfoil is modeled in tangential (tangential blowing) and perpendicular (perpendicular blowing) form and length of blowing jet is 3.5 percent of chord length. Considering previous studies, blowing jet is optimum in two distances on the airfoil surface, one around 40 percent and the other around 80 percent of chord length from the leading edge, which in this study blowing jet is placed at 80 percent of the chord length from the leading edge. Blowing velocity from 0.1 to 0.5 is considered of freestream velocity. Results of tangential blowing show that by increasing amplitude of blowing, lift and drag coefficients changes are inconsiderable. Maximum increase of lift to drag ratio in amplitude of 0.5, around 16.5 percent, but in perpendicular blowing lower amplitude of blowing is more appropriate. Also tangential blowing has no effect on stall angle and cause gradual stall of NACA 0012 airfoil, whereas perpendicular blowing improve stall angle from 14 to 16 degrees.

Keywords: Blowing, Blowing Amplitude and Coefficient, Flow Control, NACA 0012 Airfoil, Lift and Drag Coefficients.

1. INTRODUCTION

The presence of boundary layer cause major problems in different fields of fluids mechanics. However, most of studies had focused on boundary layer effects on lift and drag forces, especially on wings. Developed methods for boundary layer management, lift coefficient increase and drag coefficient reduction are known as flow separation control or boundary layer control. The scope of flow separation control on an airfoil is to achieve more lift coefficient and less drag coefficient and consequently, airfoil higher performance by increasing the lift to drag ratio. Control methods of boundary layer are divided into two categories: passive flow separation control, requiring no auxiliary power and no control loop, and active flow separation control, requiring energy expenditure. Normal uniform suction and blowing which is among passive flow separation control, has been considered in recent years and most of studies have been concentrated on oscillatory suction/blowing near leading edge. However, effects of suction/blowing parameters variation that could provide a suitable research area, hasn't been considered appropriately.

Many studies have been conducted on flow separation control. Prandtl was the first scientist who employed boundary layer suction to indicate its significant impacts on stream lines in 1904. He used suction on cylindrical surface to delay boundary layer separation. Boundary layer separation would be eliminated almost entirely by suction through a slot on the back of the cylinder [1]. First experiments on flow separation control on an airfoil were done in late 1930's to 1940. The effect of suction on boundary layer separation using slots on airfoil surface in wind tunnels was evaluated by NACA Langley memorial scientists. The first flight experiments in which seventeen suction slots were installed between 20 and 60 percent of the chord length was done. Employed airplane in this experiment was B-18 airplane [2]. Investigation on suction theoretical solution by Inverse boundary-Value problem was examined by Abzalilov et al. [3]. The efficiency of tangential unsteady suction and blowing in flow separation control on an airfoil TAU0015 was studied by Ravindran [4]. He also evaluated the effects of Zero Net Mass Flux Oscillatory Jet (Synthetic Jet) on lift coefficient increase and flight conditions in his study were Mach 0.15, Reynolds number 1.2 million at the angle of attacks 22 and 24 degree. Result showed that Lift coefficient increased from 23 percent (angle of attack 22 degree and suction coefficient is 0.0005) to 55 percent (angle of attack 24 degree and same suction coefficient). Also some researchers by analytical methods [5, 6 and 7] , experimentally [8, 9, 10, 11, 12 and 13] and some numerically [14, 15 and 16] showed that using flow separation control, such as suction, blowing and synthetic jets, causes the larger lift coefficient on thick and NACA airfoils.

Huang et al. [17] studied on flow separation control on an NACA 0012 airfoil by using suction and blowing with angle of attack 18 degree and Reynolds number of 5 Million in 2003. They proved that when jet location and angle of attack were combined, perpendicular suction at the leading edge, from 0.075 to 0.125 chord length, increased lift coefficient better than other suction situations. It has been also stated that tangential blowing at downstream locations, around 0.371 to 0.8 chord length, leads to the maximum increase in the lift coefficient value. Resendiz [18] investigated on the numerical simulation of flow separation control by oscillatory fluid injection and his result demonstrated that the use of synthetic jets on an NACA 0012 airfoil elevated the lift coefficient up to 93 percent. The application of evolutionary algorithm in order to optimize the flow separation control has been studied by Beliganur & Raymond [19] in 2007. Results of their study showed that the use of two suction jets along with two blowing jets for an NACA 0012 airfoil was able to enhance the lift to drag ratio by 12 percent. Flow separation control by synthetic jets on an NACA 0015 airfoil by using Large Eddy Simulation method was done in 2008 by You and Moin [20]. Outcomes presented that lift coefficient increased 70 percent and drag coefficient decreased 18 percent while flow separation control parameters were changed. Akcayoz & Tuncer [21] examined the optimization of synthetic jet parameters on an NACA 0015 airfoil in different angle of attack to maximize the lift to drag ratio and their results stated that optimum jet location moved toward leading edge and optimum jet angle went up while angle of attack increased. Kim et al. [22] used synthetic jets to flow separation control on an NACA 23012 airfoil. They focused on angle of attack, jet velocity and jet frequency for relatively high Reynolds numbers. This study showed, the maximum lift was obtained when the separation point coincided with the synthetic jet location and the non-dimensional frequency was one. Although the small vortex generated in the low frequency range beneficially affected the separation control and the lift enhancement, it caused the local flow structure to be easily destabilized by external disturbance or gust.

Piperas [23] in 2010 studied on flow separation control on an NACA 4415 airfoil through different suction arrangements and increased the maximum lift coefficient value by 20 percent. Genc et al. [24] studied on the numerical effects of suction and blowing on the NACA 2415 airfoil at transition zone in 2011. Although separation bubbles were not entirely eliminated in suction and blowing simulation, they either reduced or moved into the downstream. For synchronic suction and blowing, separation bubbles were exterminated completely, lift coefficient increased and drag coefficient decreased. They also showed the best results were obtained with the single suction jet, intermediate results were obtained with the multi jets and the worst results were obtained with the blowing jets. Yagiz et al. [25] worked on drag optimization on Rae5243 airfoil in transonic conditions through suction. By optimum parameters selection they increased the lift coefficient, 3.17 percent, and decreased the total drag coefficient, 3.13 percent. In addition, Yousefi et al. [26]

in 2012 reviewed the investigations on used methods in suction and blowing systems to increase or decrease drag and lift coefficient.

2. GOVERNING EQUATIONS

In this study the flow is assumed to be steady, incompressible and two-dimensional. So momentum and continuity equations become:

$$\frac{\partial u}{\partial x}+\frac{\partial v}{\partial y}=0 \tag{1}$$

$$\rho u\frac{\partial u}{\partial x}+\rho v\frac{\partial u}{\partial y}=-\frac{\partial P}{\partial x}+\frac{\partial}{\partial y}\left[\mu\left(\frac{\partial v}{\partial x}+\frac{\partial u}{\partial y}\right)\right] \tag{2}$$

$$\rho u\frac{\partial v}{\partial x}+\rho v\frac{\partial v}{\partial y}=-\frac{\partial P}{\partial y}+\frac{\partial}{\partial x}\left[\mu\left(\frac{\partial v}{\partial x}+\frac{\partial u}{\partial y}\right)\right] \tag{3}$$

The Menter's shear stress transport turbulence model ($K-\omega$ SST) was used to solve turbulence equations. This model which includes both $K-\omega$ and $K-\varepsilon$ standard models improved the calculations of boundary layer flows with separation and removed the sensitivity of $K-\omega$ model in external flows. The transport equations in Menter's shear stress turbulence model are:

$$\frac{\partial}{\partial t}(\rho k)+\frac{\partial}{\partial x_i}(\rho U_i k)=\tilde{P}_k-\beta^*\rho k\omega+\frac{\partial}{\partial x_i}\left[(\mu+\sigma_k\mu_t)\frac{\partial k}{\partial x_i}\right] \tag{4}$$

$$\frac{\partial}{\partial t}(\rho\omega)+\frac{\partial}{\partial x_i}(\rho U_i\omega)=\alpha\rho S^2-\beta\rho\omega^2+\frac{\partial}{\partial x_i}\left[(\mu+\sigma_\omega\mu_t)\frac{\partial\omega}{\partial x_i}\right]+2(1-F_1)\rho\sigma_{w2}\frac{1}{\omega}\frac{\partial k}{\partial x_i}\frac{\partial\omega}{\partial x_i} \tag{5}$$

In these equations, F_1 is blending function, S is the invariant measure of the strain rate, β^* is 0.09 and $\sigma_{\omega 2}$ is 0.856. Blending function is equal to zero away from the surface ($K-\varepsilon$ model), and switches over to one inside the boundary layer ($K-\omega$ model). A production limiter, $\widetilde{P}_k$, is used in the Menter's shear stress transport turbulence model to prevent the build-up of turbulence in stagnation regions. In addition, it is important to note that the all constants are computed by a blend from the corresponding constant of the $K-\varepsilon$ and the $K-\omega$ model via α, σ_k, σ_ω and etc [27 and 28].

$$F_1=tanh\left\{\left\{min\left[max\left(\frac{\sqrt{k}}{\beta^*\omega y},\frac{500v}{y^2\omega}\right),\frac{4\rho\sigma_{w2}k}{CD_{k\omega}y^2}\right]\right\}\right\} \tag{6}$$

$$CD_{k\omega}=max\left(2\rho\sigma_{w2}\frac{1}{\omega}\frac{\partial k}{\partial x_i}\frac{\partial\omega}{\partial x_i},10^{-10}\right) \tag{7}$$

$$P_k=\mu_t\frac{\partial U_i}{\partial x_j}\left(\frac{\partial U_i}{\partial x_j}+\frac{\partial U_j}{\partial x_i}\right) \tag{8}$$

$$\tilde{P}_k=min\,(P_k,10\beta^*\rho k\omega) \tag{9}$$

3. PARAMETERS SELECTION

In this study, the numerical code was used for simulation. Values for Reynolds number of flow and free stream velocity were 5×10^5 and 7.3037 m/s, respectively, and the used fluid was air. Geometry of NACA 0012 airfoil, blowing jet location (L_j), blowing angle (θ) and blowing jet length (h) has been shown in Figure 1. The chord length of the airfoil is 1 m and blowing slots located at 80 percent of the chord length from the leading edge. Previous studies [17] shows that blowing jet location is optimum in two distances on the airfoil surface, one around 37.1 percent and the other around 80 percent of chord length from the leading edge. Also considering previous studies [17, 18 and 21], blowing jet at the trailing edge is more appropriate of the leading edge. So in this study blowing jet is located at 80 percent of chord length from leading edge. The blowing jet

length is 3.5 percent of the chord length in tangential and perpendicular blowing and also blowing amplitude (the blowing velocity to free stream velocity ratio) considered as 0.1, 0.3 and 0.5 in experiments. Examined angles of attack also are 12, 14, 16 and 18 degrees. In our investigation, the blowing amplitude and blowing jet velocity are set as:

$$A = \frac{u_j}{u_\infty} \tag{10}$$

$$u = A.\cos(\theta + \beta) \tag{11}$$

$$v = A.sin(\theta + \beta) \tag{12}$$

Where β is the angle between free stream velocity direction and the local jet surface and θ is also the angle between the local jet surface and jet output velocity direction. Note that negative θ represents suction condition and positive θ indicates blowing condition. Since tangential and perpendicular blowing is investigated, θ is 90 and 0 degrees. Finally, blowing coefficient equals:

$$C_\mu = \frac{\rho.h.v_j^2}{\rho.C.u_\infty^2} = \frac{h}{C} \times \frac{u_j^2}{u_\infty^2} \tag{13}$$

$$H = \frac{h}{C} \tag{14}$$

$$C_\mu = H.A^2 \tag{15}$$

As it has been presented in equation (15), blowing coefficient is related to two factors: blowing amplitude (A) and blowing jet length (H). On the other hand variation of those values cause changes in suction coefficient value. Over 220 numerical simulations have been performed to cover all the cases.

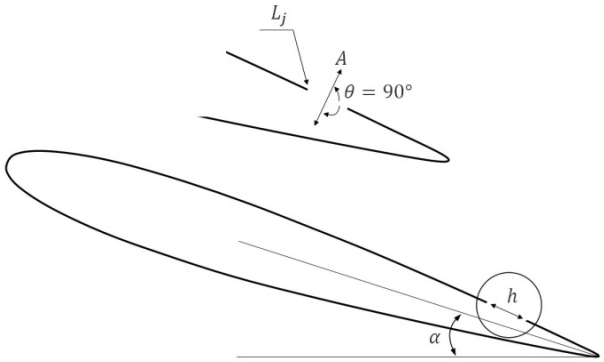

FIGURE 1: Blowing Parameters.

4. NUMERICAL SOLUTION METHOD

First and second order upwind method was employed to discretized the governing equations. First, equations are discrete by the use of first order upwind method, and the resulting system of equations is then solved using the SIMPLE method. Solution procedure is terminated when a convergence criteria of O(5) reduction in all dependent variable residuals is satisfied. Afterwards, second order upwind method was employed to discrete of equations and again, while SIMPLE method was employed to solve them. Convergence accuracy at this step is to the extent in which lift and drag coefficients fully converged, which happens usually at O(7). The key point here is that answers obtained from the first order upwind method was used as initial assumption for the second order upwind method. It is an attempt to consider the characteristics of laboratory wind tunnel, so the stream turbulence intensity is less than 0.1 percent. Airfoil computational area (C-type structured mesh) is considered as multizonal blocks in order to make structured mesh (Figure 2). The computational area grid extends from -4 chord upstream to 11 chord downstream and the upper and lower boundary extends 4 chord from the profile. In order to check the mesh

independence of the calculated results, lift and drag coefficients have been studied at angles of attack 10, 14 and 16 degrees with different size grids. Table 1 presented lift and drag coefficients at angle of attack 16 degrees and Figure 3 and 4 showed meshes independent for different angles of attack. Consequently, the grid size giving the grid independent results is selected and the total number of cells is adopted as 41,000 nodes (Table 1, Figure 3 and 4).

Number of Meshes	Lift Coefficient	Drag Coefficient
8096	0.64594	0.20889
17160	1.05134	0.12544
24480	1.09073	0.11567
40640	1.12352	0.10938
58080	1.12319	0.11187

TABLE 1: Evaluation of Mesh Independence at Angle of Attack 16 Degree.

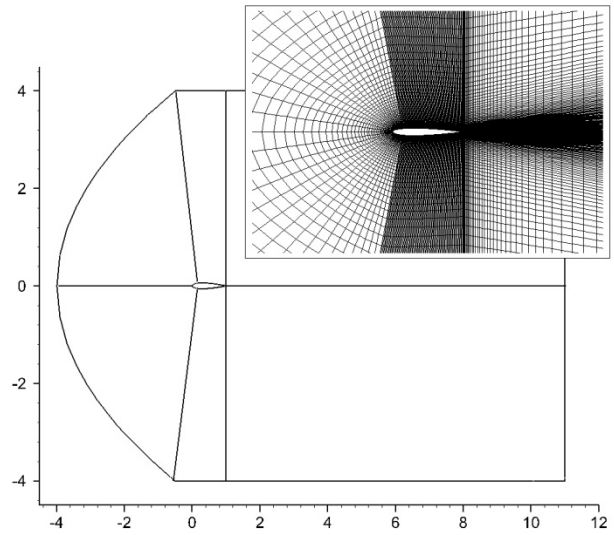

FIGURE 2: C-type Structured Mesh With Multizonal Blocks.

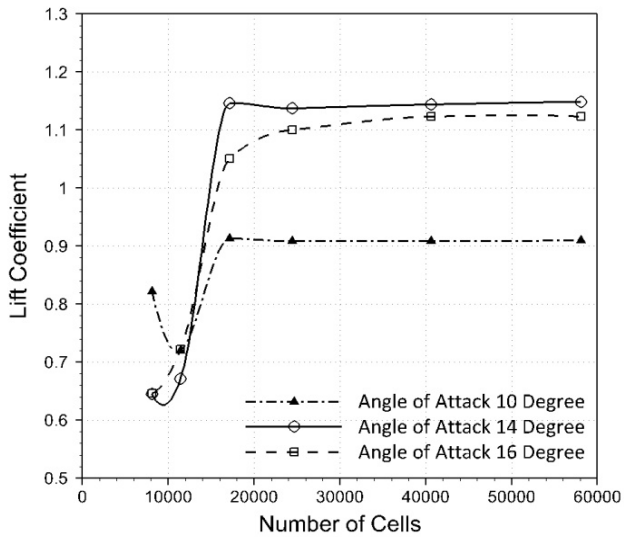

FIGURE 3: Mesh Independency For Lift Coefficient.

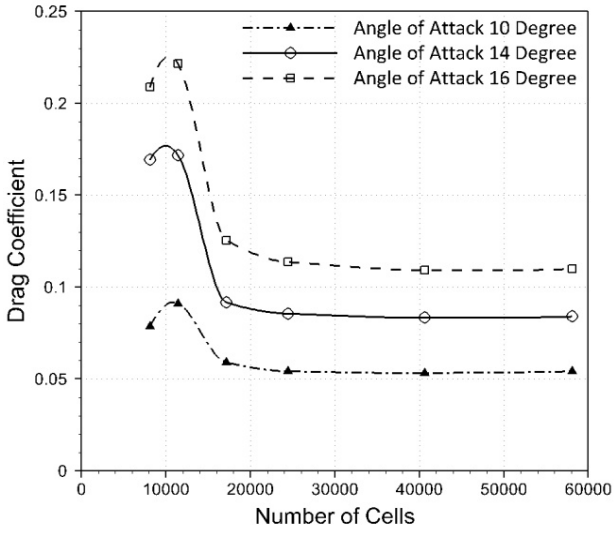

FIGURE 4: Mesh Independency For Drag Coefficient.

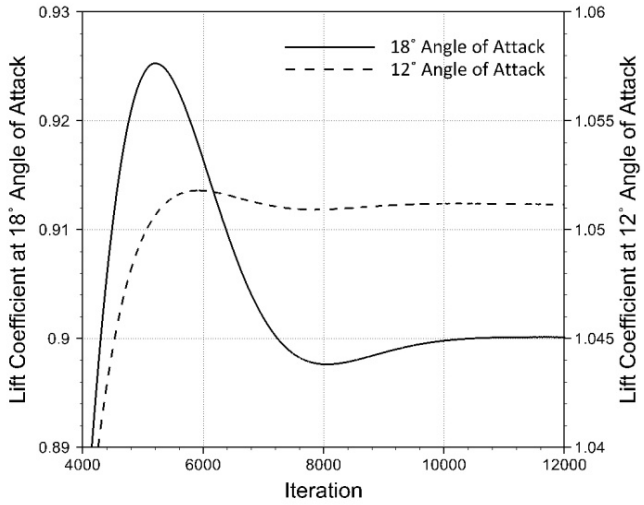

FIGURE 5: Lift Coefficient Convergence.

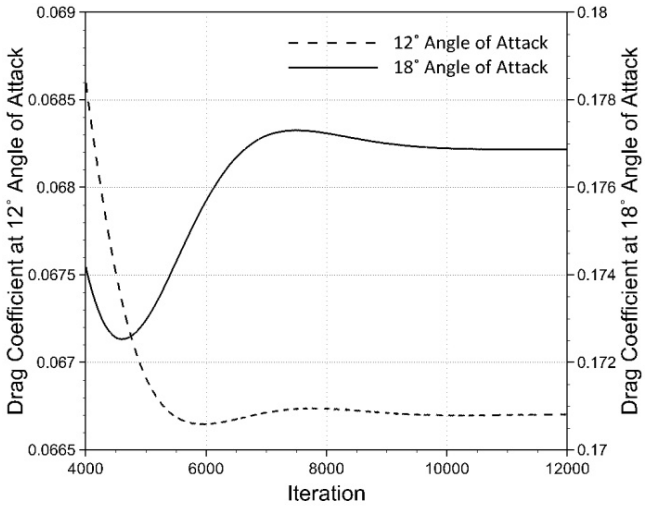

FIGURE 6: Drag Coefficient Convergence.

As demonstrated in Figure 5 and 6, the solutions in all cases, continued until lift and drag coefficient fully converged. Then, the results were compared with the results of numerical solution of Huang et al. [17] and experimental values of Critzos et al. [29] and Jacobs et al [30]. Huang et al. investigated on flow separation control using suction and blowing on NACA 0012 airfoil where the angle of attack and Reynolds number were 18 degree and 5×10^5, respectively. Parameters like jet location, suction and blowing amplitude and angle of attack were also examined by numerical method. In order to model the suction, a jet with 2.5 percent of the chord length as width was placed on the upper surface of airfoil. The GHOST code, based on finite volume, was used in this study. Critzos et al. examined aerodynamic characteristics of a NACA 0012 airfoil in laboratory experiments where Reynolds numbers were 0.5×10^5 and 1.8×10^6 and the angles of attack changed from 0 to 180 degrees. E. Jacobs et al investigated on a symmetrically NACA airfoils in wind tunnel over a wide range of the Reynolds number. The results of these four solutions are compared in Figure 7. As it is seen, computation results are near the numerical simulation of Huang et al and experimental data of Jacobs et al. The highest recorded error was 8 percent, at 14 degree angle of attack for numerical simulation and 15 percent for experimental data of Jacobs et al. Also stall angle in both method were angle of attack 14 degree. However, the results of laboratory measurements indicated that NACA 0012 airfoil stall occurs at 12 degree angle of attack. We compare our computation results at low angle of attack (less than 10 degree) with the experimental data [29, 30 and 31] in Table 2 (all experimental data at Reynolds number of 5×10^5). It can be seen that most of all the experimental data are higher than computation results. The reason can be attributed to the closer wall effects in experiment which lead to the increase of lift. It also important that turbulence model selection has a significant influence on stall angle changes. So, the selection of $K-\varepsilon$ realizable model at the same condition changes the stall angle to 16 degree. Menter's shear stress transport turbulence model always gives better results than $K-\varepsilon$ two-equation model. Prediction by $K-\varepsilon$ realizable model is quite good in the pre-stall region, while it fails to predict both the stall condition and post-stall phenomena accurately. In the $K-\varepsilon$ model, the maximum error at the angle of attack 14 degree for lift coefficient and drag coefficient were 17 percent and 25 percent, respectively. In addition, the results of performed studies showed that although Menter's shear stress transport turbulence model is more suitable model for lower Reynolds number, with larger Reynolds number $K-\varepsilon$ model gives more reliable results.

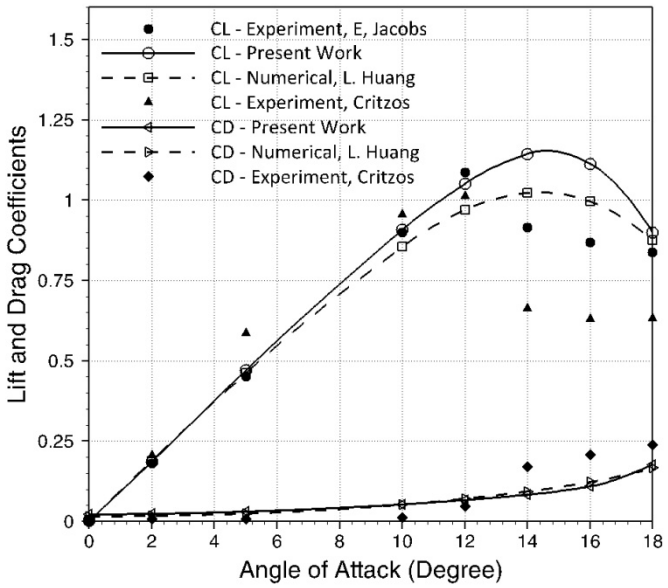

FIGURE 7: Comparison between lift and drag coefficients of present work with Huang et al. [17] numerical work and Critzos et al. [29] and Jacobs et al. [30] experimental results.

Angle of Attack	Computation Results	Experiment Critzos [29]	Experiment Jacobs [30]	Experiment Sheldahl [31]
0°	0.0021	0.0	0.0	0.0
2°	0.1853	0.2053	0.1807	0.22
5°	0.4715	0.5855	0.4511	0.55
10°	0.9087	0.9542	0.9019	1.003

TABLE 2: Comparison of computation results and experimental at angles of attack less than 10 degree.

5. RESULTS AND DISCUSSION

In the present study, first we examine tangential blowing at the trailing edge of the airfoil. Blowing slot is placed at the distance of 80 percent of the chord length from leading edge and length of blowing jet (slot) is 3.5 percent of the airfoil chord. The effect of blowing amplitude and blowing coefficient on the lift coefficient, drag coefficient and lift to drag ratio is indicated in figures 8, 9 and 10. In these figures, three blowing amplitude, 0.1, 0.3 and 0.5 with blowing coefficients of 0.00035, 0.00315 and 0.00875 are considered. By increasing blowing coefficient, lift coefficient increases a little and drag coefficient grows to 16 degree and then decreases, generally tangential blowing at the trailing edge of the airfoil increases the drag force. The effect of tangential blowing on lift and drag coefficients in angles of attack less than 10 degrees is so inconsiderable that by blowing coefficient of 0.00875 lift and drag coefficients increase only 0.5 and 5 percent respectively, but lift to drag ratio decreases about 5 percent which is unfavorable. In angles of attack less than 14 degrees (stall angle), tangential blowing causes reduction in lift to drag ratio and in angles of attack larger than 14 degrees it causes increasing. Because of this we focus on blowing effects on large angles of attack. Greatest increase of lift to drag ratio occurs in blowing coefficient of 0.00875 which increases around 16.5 percent in angle of attack of 18 degrees that in this situation lift coefficient increase by 7 percent and drag coefficient decrease by 9 percent. A considerable note about tangential steady blowing at the trailing edge of airfoil is that changes of amplitude of blowing and of blowing coefficient have very little effect on aerodynamic characteristics of NACA 0012 airfoil and increases of blowing amplitude from 0.1 to 0.3 and 0.5 cause changes less than 0.1 percent in lift and drag coefficient. This is also shown by Huang et al. [17] in tangential steady blowing near leading edge and in distance of 0.371 of chord length from leading edge. As we give energy to boundary layer by using tangential blowing, so contrary to suction [17 and 32], in blowing by increasing blowing coefficient changes of lift and drag coefficients and lift to drag ratio are almost stable.

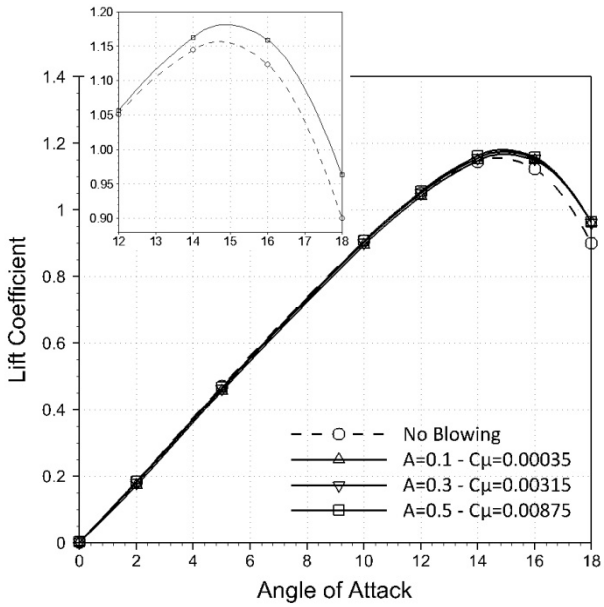

FIGURE 8: Effect of Blowing Amplitude and Blowing Coefficient On Lift Coefficient For Tangential Blowing.

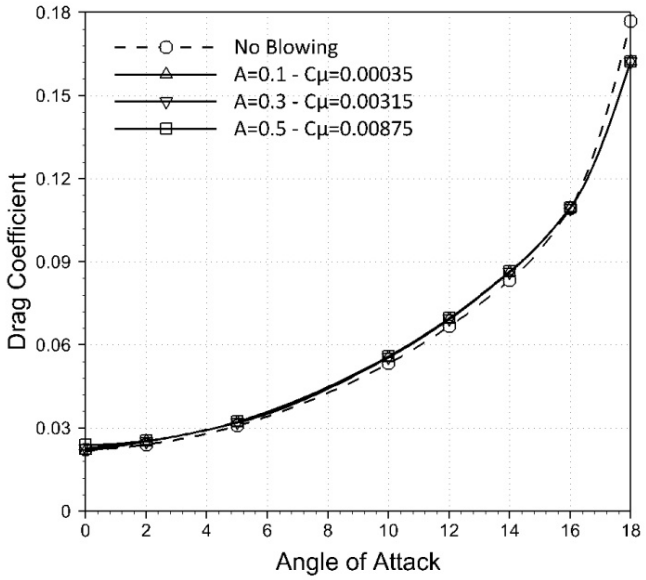

FIGURE 9: Effect of Blowing Amplitude and Blowing Coefficient Blowing On Drag For Tangential Blowing.

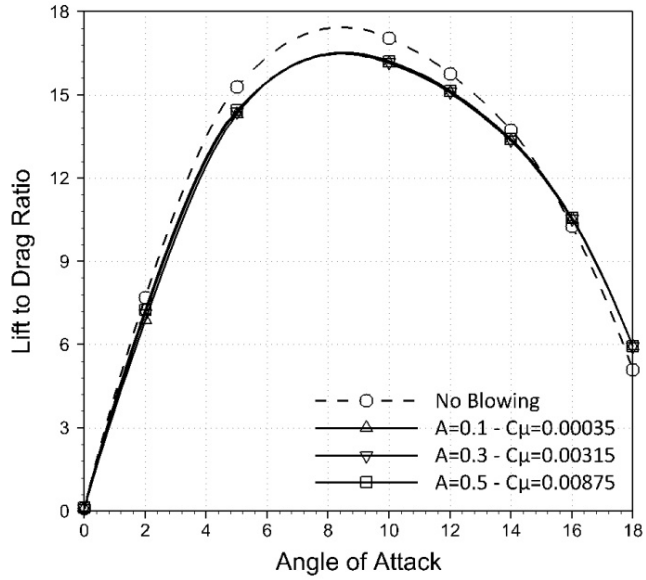

FIGURE 10: Effect of Blowing Amplitude and Blowing Coefficient On Lift To Drag Ratio For Tangential Blowing.

Another considerable note in tangential blowing is that by increasing blowing coefficient stall angle has no change and stall occur at the same angle of 14 degrees. In the airfoils it is tried to prevent sudden changes of lift coefficient after stall or sudden stall itself. Generally, airfoils with thickness of 6 to 10 percent of chord length have sudden stall and those with thickness of more than 14 percent of chord length have a gradual stall [33, 34 and 35]. Using tangential blowing results in 9 percent slower stall, however, experimental investigations show that NACA 0012 airfoil has a sudden stall [29, 30 and 31]. In our studies, lift coefficient during no-blowing situation after stall has about 10 percent decreases (lift coefficient difference percentage between angles of attack of 14 and 16 degrees), by using tangential blowing, lift coefficient has declined less than 0.4 percent. So by using steady tangent blowing as well as increasing lift to drag ratio by 16.5 percent, stall is also happening slower. On the other hand, it should be noted that by using tangential blowing separation is delayed on the airfoil. When there is no tangent blowing on the

airfoil, at the angle of attack 18 degrees, separation occurs in a distance equals to 0.103 of chord length from leading edge while by using blowing coefficient of 0.00875 separations occur in distance of 0.152 of chord length from leading edge. Streamlines around the airfoil with angle of attack 18 degrees for different blowing coefficient are shown in figure 11. As it can be seen by increasing blowing coefficient or blowing amplitude, vortexes formed at the back of airfoil are decreased but not eliminated.

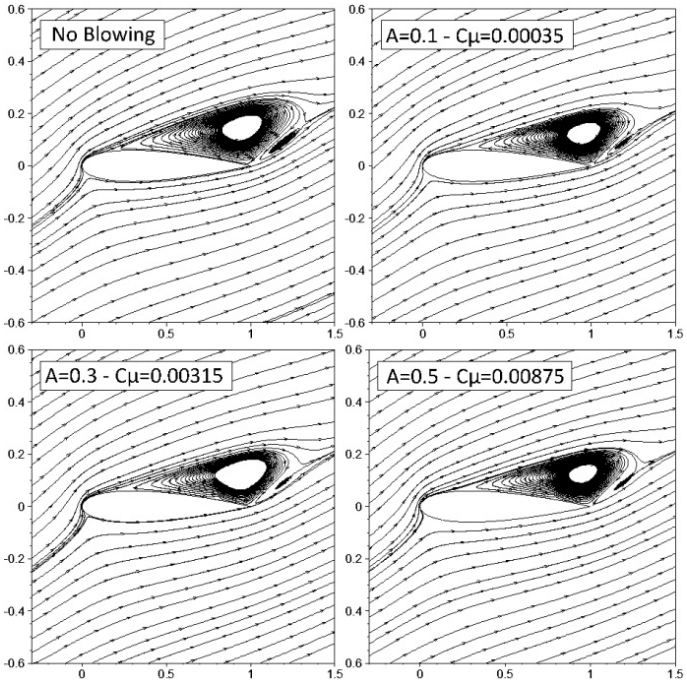

FIGURE 11: Streamlines around the airfoil with angle of attack of 18 degrees and different blowing coefficient for tangential blowing.

Thereafter we study the effect of blowing amplitude and blowing coefficient on lift and drag coefficients for perpendicular steady blowing (perpendicular blowing) at the trailing edge of NACA 0012 airfoil. Lift and drag coefficient changes and lift to drag ratio changes with angles of attack in blowing amplitudes of 0.1, 0.3 and .05 are shown in figures 12, 13 and 14. In perpendicular blowing, contrary to tangential blowing, the increase of amplitude and/or blowing coefficient make the condition worse so that using blowing amplitude of 0.1 in angle of attack 14 degrees decreases lift to drag ratio by 6.5 percent and using blowing amplitude of 0.5 decreases lift to drag ratio by 17 percent. Generally, using perpendicular blowing makes the situation worse, before stall angle perpendicular blowing decrease lift to drag ratio intensively and after stall and in angle of attack of 18 degrees cause 25 percent increase in lift to drag ratio. Blowing increase the boundary layer momentum [36] and turbulence is increased by the energy added to the boundary layer by perpendicular blowing, so the more blowing amplitude or blowing coefficient increases, the larger are the turbulence of flow and vortex and eventually the more lift to drag ratio decreases. In figure 15 tangential and perpendicular steady blowing in angles of attack 16 and 18 degrees and blowing amplitude of 0.5 are compared. As it can be seen, perpendicular blowing at the trailing edge of airfoil causes larger vortexes. There is two substantial points in controlling the flow separation in perpendicular blowing at the end of the airfoil, first by using perpendicular blowing stall angle changes from 14 to 16 degrees, and second by increasing angle of attack influence percent of perpendicular blowing goes up and even in angle of attack 18 degrees results in 25 percent increase of lift to drag ratio. Changes of lift to drag ratio with blowing amplitude of 0.1 compared to no blowing status are shown in table 3.

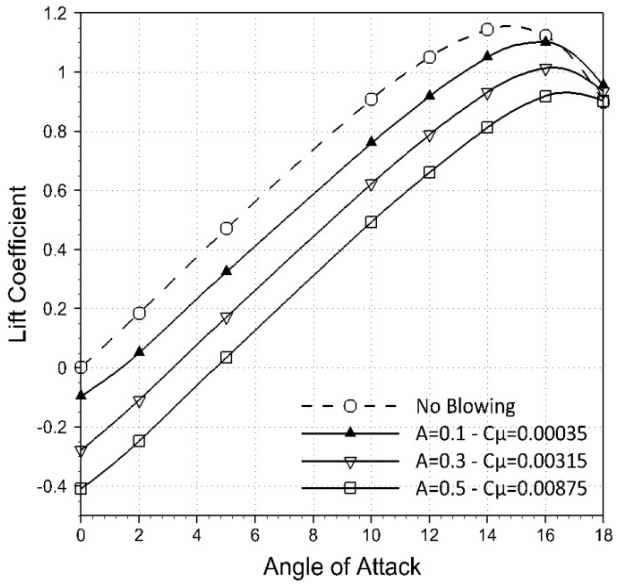

FIGURE 12: Effect of Blowing Amplitude and Blowing Coefficient On Lift Coefficient For Perpendicular Blowing.

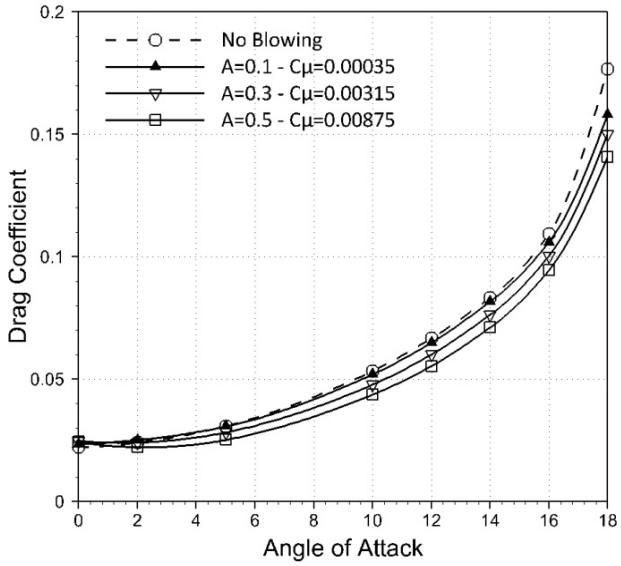

FIGURE 13: Effect of Blowing Amplitude and Blowing Coefficient On Drag Coefficient For Perpendicular Blowing.

Angle of Attack	Lift Coefficient	Drag Coefficient	Percent of Lift to Drag Ratio Increase/Decrease
10˚	0.76067	0.05197	16.5 percent decrease
12˚	0.91897	0.06488	11.2 percent decrease
14˚	1.05061	0.08167	6.71 percent decrease
16˚	1.10173	0.10589	1.23 percent decrease
18˚	0.95459	0.15812	18.6 percent increase
20˚	0.68146	0.27497	3.31 percent increase

TABLE 3: Changes of lift to drag ratio with blowing amplitude of 0.1 compared to no blowing situations in different angles of attack.

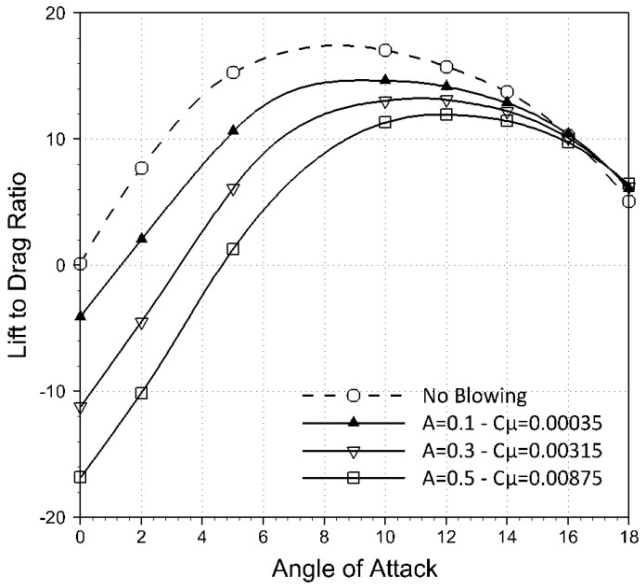

FIGURE 14: Effect of Blowing Amplitude and Blowing Coefficient On Lift To Drag Ratio For Perpendicular Blowing.

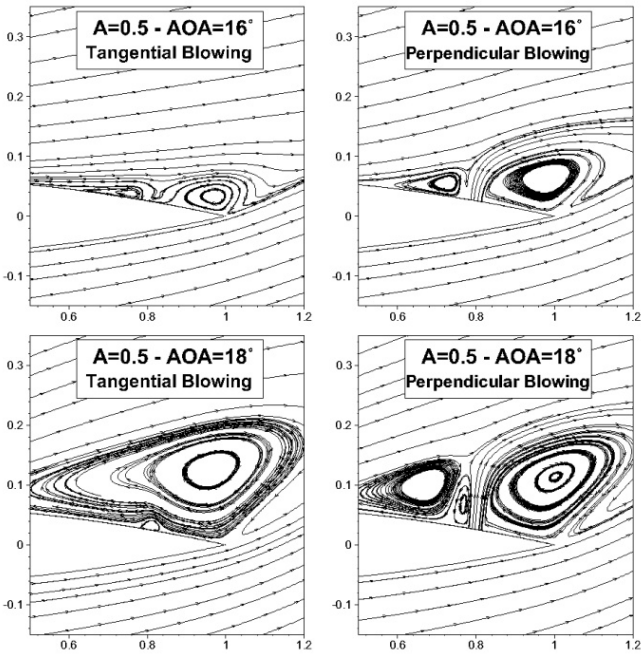

FIGURE 15: Comparing Tangential and Perpendicular Steady Blowing.

6. CONCLUSION

In this study the effects of tangential and perpendicular steady blowing on NACA 0012 airfoil are examined and analyzed to flow separation control. To do this the effect of changing parameters of blowing amplitude and blowing coefficient are modeled numerically and following results are gained. In tangential blowing by increasing blowing amplitude lift to drag ratio grows and separation point is transferred downstream, while increasing blowing amplitude makes situation worse in perpendicular blowing and causes larger vortexes. In other words, in perpendicular blowing smaller value of blowing amplitude or blowing coefficient are more appropriate. In

tangential blowing greatest increase of lift to drag ratio occur in blowing amplitude of 0.5 and blowing coefficient of 0.00875 which in this situation and with angle of attack 18 degrees, airfoil back vortexes are declined. On the other hand, using perpendicular blowing makes situation worse than no blowing status. Results showed that in small angles of attack flow separation control by using blowing has no favorable effect on aerodynamics characteristics. Also using tangential blowing on airfoil causes no change in airfoil stall angle but results show slower stall, but perpendicular blowing changes airfoil stall angle from 14 to 16 degrees.

Also, in this numerical simulation the maximum lift coefficient increase by 7 percent and lift to drag ratio increase by 16.5 percent for tangential blowing, in blowing coefficient of 0.00875, blowing amplitude of 0.5 and 18 degree angle of attack. Perpendicular blowing was useful just for angles of attack larger than stall angle, in the situation of blowing coefficient of 0.00875, blowing amplitude of 0.5 and 18 degree angle of attack, lift to drag ratio increase by 18.5 percent.

7. FUTURE RESEARCH DIRECTIONS

Although several studies have been carried out experimentally and numerically on suction and blowing on the airfoil, some important suction and blowing parameters like the number of suction and blowing slots, slot arrangements, slots entrance or exit angle, oscillatory suction and blowing and also synthetic jet parameters have been not fully examined. Laboratory studies on suction and blowing parameters are limited and the majority of previous investigations have been performed on the streams with low Reynolds numbers. Therefore, future studies could be concentrated on flows with high Reynolds numbers.

8. REFERENCES

[1] M. Gad-el-hak. Control Flow: Passive, Active and Reactive Flow Management. United Kingdom: Cambridge University Press, 2000, pp. 25-35.

[2] A.L. Braslow, “A History of Suction Type Laminar Flow Control with Emphasis on Flight Research,” NASA History Division, Monograph in Aerospace History, Number 13, 1999.

[3] D.F. Abzalilov, L.A. Aksentev and N.B. IL’Inskii, “The Inverse Boundary-Value Problem for an Airfoil with a Suction Slot,” Journal of Applied Mathematics and Mechanics, Vol. 61, pp. 75-82, 1997.

[4] S.S. Ravindran, “Active Control of Flow Separation Over an Airfoil,” Report of Langley Research Center, 1999.

[5] M.B. Glauert, “The Design of Suction Aerofoils with a Very Large C_L-Range,” Aeronautical Research Council, R&M 2111, 1945.

[6] M.B. Glauert, W.S. Walker, W.G. Raymer and N. Gregory, “Wind Tunnel Tests on a Thick Suction Airfoil with a Single Slot,” Aeronautical Research Council, R&M 2646, 1948.

[7] M.B. Glauert, “The Application of the Exact Method of Aerofoil Design,” Aeronautical Research Council, R&M 2683, 1947.

[8] S. Dirlik, K. Kimmel, A. Sekelsky and J. Slomski, “Experimental Evaluation of a 50-Percent Thick Airfoil with Blowing and Suction Boundary Layer Control,” AIAA Paper, Vol. 92, 1992.

[9] D.M. Heugen, “An Experimental Study of a Symmetrical Aerofoil with a Rear Suction Slot and a Retractable Flap,” Journal of Royal Aeronautical Society, Vol. 57, 1953.

[10] H.J. Howe and B.J. Neumann, “An Experimental Evaluation of a Low Propulsive Power Discrete Suction Concept Applied to an Axisymmetric Vehicle,” David W. Taylor Naval Ship R&D Center TM 16-82/02, 1982.

[11] J.H. Preston, N. Gregory and A.G. Rawcliffe, “The Theoretical Estimation of Power Requirements for Slot-Suction Aerofoils with Numerical Results for Two Thick Griffith Type Sections,” Aeronautical Research Council, R&M 1577, 1948.

[12] E.J. Richards, and C.H. Burge, “An Airfoil Designed to Give Laminar Flow Over the Surface with Boundary Layer Suction,” Aeronautical Research Council, R&M 2263, 1943.

[13] E.J. Richards, W.S. Waler and C.R. Taylor, “Wind Tunnel Tests on 30-Percent Suction Wing,” Aeronautical Research Council, R&M 2149, 1945.

[14] D.P. Rizzetta, M.R. Visbal and M.J. Stank, “Numerical Investigation of Synthetic Jet Flow Fields,” AIAA Journal, Vol. 37, pp. 919-927, 1999.

[15] J.Z. Wu, X.Y. Lu, A.G. Denny, M. Fan and J.M. Wu, “Post-Stall Flow Control on an Airfoil by local Unsteady Forcing,” Journal of Fluid Mechanics, Vol. 371, PP. 21-58, 1998.

[16] C. Nae, “Synthetics Jets Influence on NACA0012 Airfoil at High Angle of Attacks,” AIAA Papers, PP. 98, 1998.

[17] L. Huang, P.G. Huang and R.P. LeBeau, “Numerical Study of Blowing and Suction Control Mechanism on NACA0012 Airfoil,” Journal of Aircraft, Vol. 41, No. 1, 2004.

[18] C.R. Rosas, “Numerical Simulation of Flow Separation Control by Oscillatort Fluid Injection,” Doctor of Philosophy Thesis, A&M University, Texas, 2005.

[19] N.K. Beliganur and P. Raymond, “Application of Evolutionary Algorithms to Flow Control Optimization,” Report of University of Kentuchky, 2007.

[20] D. You and P. Moin, “Active Control of Flow Separation Over an Airfoil Using Synthetic Jets,” Journal of Fluids and Structures, Vol. 24, pp. 1349-1357, 2008.

[21] E. Akcayoz and I.H. Tuncer, “Numerical Investigation of Flow Control Over an Airfoil Using Synthetic Jets and its Optimization,” International Aerospace Conference, Turkey, 2009.

[22] S.H. Kim and C. Kim, “Separation Control on NACA23012 Using Synthetic Jet,” Aerospace Science and Technology, Vol. 13, pp.172-182, 2009.

[23] A.T. Piperas, “Investigation of Boundary Layer Suction on a Wind Turbine Airfoil Using CFD,” Master Thesis, Technical University of Denmark, Denmark, 2010.

[24] M.S. Genc, U. Keynak and H. Yapici, “Performance of Transition Model for Predicting Low Re Aerofoil Flows Without/With Single and Simultaneous Blowing and Suction,” European Journal of Mechanics B/Fluids, Vol. 30, pp. 218-235, 2011.

[25] B Yagiz, O. Kandil and Y. V. Pehlivanoglu, “Drag Minimization Using Active and Passive Flow Control Techniques,” Aerospace Science and Technology, Vol. 17, pp. 21-31, 2011.

[26] K. Yousefi, S.R. Saleh and P. Zahedi, “Investigation for Increase or Decrease The Lift and Drag Coefficient on The Airfoil with Suction and Blowing,” International Conference on Mechanical Engineering and Advanced Technology, Iran, 2012.

[27] F.R. Menter, M. Kuntz and R. Langtry, “Ten Years of Industrial Experience with the SST Turbulence Model,” 4th International Symposium on Turbulence, Heat and Mass Transfer, Turkey, 2003.

[28] L.K. Voigt, J.N. Sorensen, J.M. Pedersen and M. Crons, “Review of Four Turbulence Models Using Topology,” 8th International IBPSA Conference, Netherlands, 2003.

[29] C.C. Critzos, H.H. Heyson and W. Boswinkle, “Aerodynamics Characteristics of NACA0012 Airfoil Section at Angle of Attacks from 0° to 180°,” Langley Aeronautical Laboratory, Washington, NACA Technical Note 3361, 1955.

[30] E. Jacobs and A. Sherman, “Airfoil Section Characteristic as Affected by Variations of the Reynolds Number”, NACA Report 586,231, 1937.

[31] R.E. Sheldhal and Klimas, ‘‘Aerodynamic Characteristics of Seven Airfoil Sections Through 180 Degrees Angle of Attack for use In Aerodynamic Analysis of Vertical Axis Wind Tunnel’’, Sandia National Labs., Report No. SAND80-2114, Albuquerque, March 1981.

[32] M. Goodarzi, R. Fereidouni and M. Rahimi, “Investigation of Flow Control Over a NACA 0012 Airfoil by Suction Effect on Aerodynamic Characteristics”, Canadian Journal of Mechanical Sciences and Engineering, Vol.3, No.3, pp. 102-108, 2012.

[33] I.H. Abbott and A.E. Von Doenhoff. Theory of Wing Sections. Dover, 1959.

[34] R. Eppler. Airfoil Design and Data. Springer, 1990.

[35] J. Olejniczak and A.S. Lyrintzis, “Design of Optimized Airfoils in Subcritical Flow”, Journal of Aircraft, Vol. 31, No. 30, pp. 680-687, 1994.

[36] A. Seifert, A. Darabi and I. Wygnansky, “Delay of Airfoil Stall by Periodic Extinction”, Journal of Aircraft, Vol. 33, pp. 691-698, 1996.

Advantages and Disadvantages of Using MATLAB/ode45 for Solving Differential Equations in Engineering Applications

Waleed K. Ahmed *w.ahmed@uaeu.ac.ae*
Faculty of Engineering/ Engineering Requirements Unit
UAE University
Abu Dhabi, Al-Ain, 15551, UAE

Abstract

The present paper demonstrates the route used for solving differential equations for the engineering applications at UAEU. Usually students at the Engineering Requirements Unit (ERU) stage of the Faculty of Engineering at the UAEU must enroll in a course of Differential Equations and Engineering Applications (MATH 2210) as a prerequisite for the subsequent stages of their study. Mainly, one of the objectives of this course is that the students practice MATLAB software package during the course. The aim of using this software is to solve differential equations individually and as a system of equation in parallel with analytical mathematics trends. In general, mathematical models of the engineering systems like mechanical, thermal, electrical, chemical and civil are modeled and solve to predict the behavior of the system under different conditions. The paper presents the technique which is used to solve DE using MATLAB. The main code that utilized and presented is MATLAB/ode45 to enable the students solving initial value DE and experience the response of the engineering systems for different applied conditions. Moreover, both advantages and disadvantages are presented especially the student mostly face in solving system of DE using ode45 code

Keywords: Advantages, DE, Disadvantages, Engineering, MATLAB, ode45.

1. INTRODUCTION

Engineering software is one of the most important tools in engineering education and they can be very useful in teaching the working principles of various engineering instruments and devices [1]. Usually differential equations can be used for solving different applications of engineering fields like electrical, mechanical, civil and chemical besides to the petroleum engineering. Normally, at the early stages of their study in the faculty of engineering at UAEU, a considerable amount of time and efforts are needed by the students to solve the differential equations of the mathematical models of different engineering systems especially the dynamic systems [2]. In general, students experience applied differential equations through the engineering applications whereas involved with the classical math solution through the mathematic lecture. One of the objectives of the course MATH 2210 is to let students practice solving applied differential equations of the engineering cases [3]. Generally, the mathematical solution of these equations does not readily which provides the student with a graphical image of the anticipated results, since they deal with different style of the mathematical models depending on the case studied itself. As a result, the students are uncomfortable with the entire process of solving these types of systems [4].

As a matter of fact, writing a program from first principles is not an easy task and needs considerable programming skills [1]. Mainly programs are developed using a high-level programming language such as FORTRAN, C++, PASCAL or BASIC to solve the differential equations. The advantages and disadvantages of writing a simulation program can be summarized as following:

• Requires excellent programming skills
• Takes long time to develop and test
• Very cheap as the existing compilers can be used for development.
• Source code is available, so it can be modified and upgraded at no cost.
• The program is usually written for a dedicated simulation problem.

An alternate option of solving engineering system is to use a commercially available simulation package. Using this option can be classified into two categories: general simulation packages, and dedicated simulation packages. General simulation packages can be used to simulate and solve most of the engineering of different fields, such as Excel [5], MATLAB [6], MatriXx [7], and so on. The advantages and disadvantages of general simulation packages are:

• Affordable cost.
•No Programming skills are required.
• Relatively easy to simulate and generate results.
• It is necessary to get the mathematical model of simulated system and this may be difficult to handle.
• The source code is not available and hence it is not possible to modify/upgrade the simulation package.

MATLAB is a computer program that provides the user with a convenient environment for performing many types of calculations [8]. Besides it is usually used to solve differential equations and it is an effective way and can be considered as quick and easy. Moreover, it may also provide the student with the symbolic solution and a visual plot of the result. One of the most popular codes used to solve differential equation is ode45, which is mainly used for solving engineering applications of the MATH2210. Dealing with diverse engineering applications can result different order of differential equations, besides the engineering system it may result a system of differential equation whether the system has the same style of DE or mixed order DE. This can cause a sort of complication toward writing the MATLAB program which is dedicate to predict the behavior of the engineering case studied.

In this paper, a different system of differentials equations which express the mathematical model of diverse applications [9] is inspected to test the differences in the solution by MATLAB using the ODE45 code technique instead of using numerical analysis technique. This will clarify the advantages and disadvantages of the code used. Mainly three cases are demonstrated, the first order differential equation which represented by the thermal system and the second order differential equation which is practiced through mechanical system and eventually the mixed order of differential equations which is mostly encountered by the electrical applications.

2. FIRST ORDER DIFFERENTIAL EQUATIONS OF THERMAL SYSTEM

One of the first engineering applications that always students practice in the MATH 2210 course is the thermal system [10]. The aim of this application is to start with a single first order differential equation and as well as a system of equations. Unusually this system generates a mathematical model in term of first order and this is because the rate of change of temperature. As an example Consider the closed vessel of thermal resistance R_{La} which is filled with liquid that contains an electrical heater immersed in the liquid. The heater is contained within a metal jacket of thermal resistance R_{HL}. The heater has a thermal capacitance of C_H, and the liquid has a thermal capacitance of C_L. The heater temperature is Θ_H, and the liquid temperature is Θ_L. The heater is supplying energy at a rate of qi(t), and the exterior temperature is Θ_a. The objective is to find the system mathematical model in terms of $\Theta_H(t)$, $\Theta_L(t)$ which represents the temperature variation with respect to time. The present case is modeled by a couple of DE derived from the heat transfer principles [10]. The mathematical model is shown below:

$$\dot{\theta}_H(t) = \frac{1}{C_H}\left[q_i(t) - \frac{1}{R_{HL}}\left(\dot{\theta}_L(t) - \theta_L(t)\right)\right] \quad (1)$$

$$\dot{\theta}_L(t) = \frac{1}{C_L}\left[\frac{1}{R_{HL}}\left(\theta_H(t) - \theta_L(t)\right) - \frac{1}{R_{La}}\left(\theta_L(t) - \theta_a\right)\right] \quad (2)$$

This can be written in matrix form:

$$\begin{bmatrix} \dot{\theta}_H(t) \\ \\ \dot{\theta}_L(t) \end{bmatrix} = \begin{bmatrix} \frac{1}{C_H R_{HL}} & \frac{-1}{C_H R_{HL}} \\ \frac{1}{C_L R_{HL}} & \frac{-1}{C_L R_{HL}} - \frac{1}{C_L R_{La}} \end{bmatrix} \begin{bmatrix} \theta_H(t) \\ \\ \theta_L(t) \end{bmatrix} + \begin{bmatrix} q_i(t) \\ \\ \frac{\theta_a}{R_{La}} \end{bmatrix} \quad (3)$$

In compact form this is represented by [3]:

$$\dot{x} = Ax + Bu \quad (4)$$

$$x^{\bullet} = \begin{bmatrix} \dot{\theta}_H(t) \\ \\ \dot{\theta}_L(t) \end{bmatrix}, \mathrm{A} = \begin{bmatrix} \frac{1}{C_H R_{HL}} & \frac{-1}{C_H R_{HL}} \\ \frac{1}{C_L R_{HL}} & \frac{-1}{C_L R_{HL}} - \frac{1}{C_L R_{La}} \end{bmatrix} \quad (5)$$

$$\mathrm{x} = \begin{bmatrix} \theta_H(t) \\ \\ \theta_L(t) \end{bmatrix}, B = \begin{bmatrix} q_i(t) \\ \\ \frac{\theta_a}{R_{La}} \end{bmatrix} \quad (6)$$

One of the features that ode45 solver requires is that the system of equations must be in first order differential equations [8], and this is already generated by the thermal system mathematical model. Therefore it will be straight forward to program the code necessary for the solution as shown below without any complication, only needed is to form the mathematical model to be accepted by the code. The program for the mathematical model is shown below.

```
Clear;clc
[t,theta] = ode45('ThermalEx3',[0 1000],[300 300]);
plot(t,theta(:,1),t,theta(:,2))

function dthetadt = ThermalEx3(t,theta)
RHL=1e-3; CH=20e3;
RLa=5e-3; CL=1e6;
thetaa=300;qi=2500;
eq1=[-(1/(RHL*CH))*theta(1)+(1/(RHL*CH))*theta(2)+(1/CH)*qi];
eq2=[-((1/(RHL*CL))+(1/(RLa*CL)))*theta(2)+(1/(RHL*CL))*theta(1)+(1/(RLa*CL))*thetaa];
dthetadt =[eq1;eq2];
```

3. SECOND ORDER DIFFERENTIAL EQUATIONS OF MECHANICAL SYSTEM

Usually the mathematical model of mechanical engineering systems is in the form of second order differential equation, and that because of the Newton's second law. In this example, a mass-spring-damper is modeled and then its behavior is simulated [11]. The system consists of a mass (m), a spring (k), and a damper (C). An external force (f) is applied on the mass. The system can easily be simulated and its response can be plotted as a function of time. Before the system can be simulated it is necessary to derive its mathematical model. The mathematical model of mechanical systems usually has the following form:

$$Mx''+Cx'+kx=f(t) \tag{7}$$

For the above system, simple there are two approaches can be easily used to solve the mathematical model using MATLAB. In this paper both ODE45 code as the technique that the students learn through the lectures. Unfortunately using ODE45 is not straight forward way to solve a second order differential equation, so a modification must be done by the students to be suitable for the code utilization and solution. By reorganizing a single second order differential to a couple of first order differential equation by defining a new system of variables [12], the new system will be quite fit for the ode45 code for the solution. In particular, if a new variables z_1 and z_2 are introduced such that:

$$z_1=x \quad \text{and} \quad z_2=x' \tag{8}$$

These implies that

$$z'_1=z_2\ ,\ z'_2= x'' \tag{9}$$

Then the model can be written as:

$$m.z_2'+C.z_2+k.z_1=f(t) \tag{10}$$

Next solve for z_2' to get:

$$z_2'=1/m\ (f(t)-C.z_2-k.z_1) \tag{11}$$

Equations (3) and (4) constitute a state variable model corresponding to the reduced model. The variables z_1 and z_2 are the state variables. The choice of the state variable is not unique, but the choice must result in a set of first order differential equations, and a consequence the situation will be more complicated when dealing with more than single equation, and this is one of the most problems that the students face in this stage. The state variable equation can be written in matrix form as follows:

$$\begin{bmatrix} \dot{z}_1 \\ \dot{z}_2 \end{bmatrix} = \begin{bmatrix} 0 & 1 \\ -\frac{k}{m} & -\frac{C}{m} \end{bmatrix} \begin{bmatrix} z_1 \\ z_2 \end{bmatrix} + \begin{bmatrix} 0 \\ \frac{1}{m} \end{bmatrix} u(t) \tag{12}$$

In compact form this can be represented by:

$$A = \begin{bmatrix} 0 & 1 \\ -\frac{k}{m} & -\frac{C}{m} \end{bmatrix} \quad B = \begin{bmatrix} 0 \\ \frac{1}{m} \end{bmatrix} \quad z = \begin{bmatrix} z_1 \\ z_2 \end{bmatrix} \tag{13}$$

The mechanical system can now be solved the using the MATLAB package. The MATLAB function developed to simulate the system and plot the displacement and velocity of the system. The component values can easily be changed and the system can be re-simulated. In this example, the following component values were chosen for the simulation: m=1 kg, C=2 N.s/m, k=1000 N/m, initial displacement (Xo)=0.5 m, initial velocity(Vo)=0.2 m/s, force(f)=50*sin(2t).

```
function dzdt = Mech(t,z)
m=1;
k=100;
C=2;
dzdt = [ z(2); (1/m)*(50*sin(2*t)-C*z(2)-k*z(1)) ];

[t, z] = ode45('Mech',[0,20],[0.5; 0.2]);
plot(t, z)
```

4. MIXED ORDER DIFFERENTIAL EQUATIONS

The code for a first-order ODE is very straightforward. However, a second or third order ODE cannot be directly used. You must first rewrite the higher order ODE as a system of first-order ODEs that can be solved with the MATLAB ODE solvers [13].

This is an example of how to reduce a second-order differential equation into two first order equations for use with MATLAB ODE solvers such as ODE45. The following system of equations consists of one first and one second-order differential equations:

$$x' = -y * \exp(-t/5) + y' * \exp(-t/5) + 1 \quad (14)$$
$$y'' = -2*\sin(t) \quad (15)$$

By assuming $z_1=x$, the first step is to introduce a new variable that equals the first derivative of the free variable in the second order equation $z_2=y$ and $z_3=y'$. Taking the derivative of each side yields the following:

$$z_2'=y'=z3 \quad (16)$$
$$z_3' = y'' \quad (17)$$

Substituting (17) into (15) produces the following:

$$z_3' = -2*\sin(t) \quad (18)$$

Combining (14), (16), and (18) yields three first order differential equations.

$$z_1' = -y * \exp(-t/5) + y' * \exp(-t/5) + 1; \quad (19)$$
$$z_2' = y' \quad (20)$$
$$z_3' = -2*\sin(t) \quad (21)$$

Since $z_3 = y'$, substitute z_3 for y' in equation (19). Also, since MATLAB requires that all derivatives are on the left hand side, rewrite equation (20). This produces the following set of equations:

$$z_1' = -z_2 * \exp(-t/5) + z3 * \exp(-t/5) + 1 \quad (22)$$
$$z_2' = z_3 \quad (23)$$
$$z_3' = -2*\sin(t) \quad (24)$$

The matrix form of the final system of equations is shown by:

$$\begin{bmatrix} z1' \\ z2' \\ z3' \end{bmatrix} = \begin{bmatrix} 0 & -\exp(-t/5) & \exp(-t/5) \\ 0 & 0 & 1 \\ 0 & 0 & 0 \end{bmatrix} \begin{bmatrix} z1 \\ z2 \\ z3 \end{bmatrix} + \begin{bmatrix} 1 \\ 0 \\ -2 * \sin(t) \end{bmatrix} \quad (23)$$

To evaluate this system of equations using ODE45 or another MATLAB ODE solver, create a function that contains these differential equations. The function requires two inputs, the states and time, and returns the state derivatives.

Following is the MATLAB code needed for the solution to evaluate the system of equations using ODE45 or another MATLAB ODE solver. Define the start and stop times and the initial conditions of the state vector:

```
function xprime = odetest(t,z)
eq1 = -z(2) * exp(-t/5) + z(3) * exp(-t/5) + 1;
eq2 = z(3);
eq3 = -2*sin(t);
xprime = [eq1;eq2;eq3];

clc
clear
t0 = 5;
tf = 20; x0 = [1 -1 3] % Initial conditions
[t,z] = ode45('odetest',[t0,tf],x0);
plot(t,z)
```

Unfortunately this case mostly can be faced in the electrical applications and this cause complication especially if the mathematical model contain a system of equations and hence the probability of the mistakes through the transformations stages is very high and will be reflected on the final results and not forgetting the time consumed. Instead SIMULINK [14] can be used as an alternate option for the engineering applications.

5. CONCLUSIONS

The present paper shows that dealing with differential equations of the mathematical models of engineering systems mostly encounter difficulties in term of the MATLAB programming. As a matter of fact this complication is due to restrictions of the ode45 which is mostly used to solve such kind of differential equations. Few systems like thermal system are in the form of first order differential equations which are quite fit with requirements of the ode45. The major restriction of the MATLAB solve code is that the system of differential equations should be organized in the form of the first order differential equations, and this frequently is a rare case, whereas the core engineering application either in the form of second order of even mixed order. Therefore, transformation of the system of differential equations is mandatory, and this can make mistakes beside to the time spent.

6. REFERENCES

[1] D. Ibrahim. “Engineering simulation with MATLAB: improving teaching and learning effectiveness”. Procedia Computer Science 3, 2011, pp. 853–858.

[2] G.F. Simmons and S.G. Krantz. “Differential Equations: Theory, Techniques, and Practice”, International Edition, New York: McGraw Hill, 2007.

[3] P.V. O'Neil. “Advanced Engineering Mathematics”, International Student Edition, Ontario: Thomson, 1995.

[4] F. Pietryga. “Solving Differential Equations Using MATLAB/Simulink”, Proceedings of the American Society for Engineering Education Annual Conference & Exposition, 2005.

[5] J. Walkenbach. “Excel 2007 Bible”, Indianapolis: John Wiley & Sons, 2007.

[6] B. Hahn, D. Valentine. "Essential Matlab for Engineers and Scientists", 4th edition, MA: Academic Press, 2007.

[7] MatriXx Software Suite, National Semiconductors, web site: http://www.ni.com .

[8] S.C. Chapra. "Applied Numerical Methods with MATLAB", 2nd ed., New York: McGraw Hill, ,2008.

[9] D. Zill. "A First Course in Differential Equations with Modeling and Applications", Brooks/Cole Publishing Company, 6th ed, 1997.

[10] C. Close, D. Frederick, J. Newell. "Modeling and Analysis of Dynamic Systems", John Wiley and Sons, Inc., 3rd ed, 2002.

[11] K. Ogata. "System Dynamics", 4th ed., New Jersy: Pearson Prentice Hall, 2004.

[12] W.J. Palm. "System Dynamics", International 2nd Edition, New York: McGraw Hill, 2010.

[13] http://www.mathworks.com/support/tech-notes/1500/1510.html.

[14] W.Ahmed, K.Harib, "MATLAB/SIMULINK to Solve Mathematical Models of Engineering Systems: Class Activity", ICERI2011, Proceedings of the 4th International Conference of Education, Research and Innovation, Madrid, Spain, 14-16 November, 2011. ISBN: 978-84-615-3324-4.

Development of Modified Evaluation and Prioritization of Risk Priority Number in FMEA

N. Sellappan *sanov18@yahoo.com*
Faculty of Engineering/Mechanical and Industrial Engineering Section
Salalah College of Technology, P. B. No. 608
Salalah, Postal Code: 211, Sultanate of Oman

K. Palanikumar *palanikumar_k@yahoo.com*
Faculty of Mechanical Engineering
Sri Sai Ram Institute of Technology
Chennai - 44, Tamil Nadu, India

Abstract

Failure Mode and Effects Analysis (FMEA) is a tool used for identifying, analyzing and prioritizing failure modes of a product and process. The traditional FMEA determines the risk priority of each failure mode using the risk priority number (RPN) by multiplying the ranks of the three risk factors namely the Severity (S), Occurrence (O) and Detection (D). FMEA is carried out by a team of members and the critical problem is that the team often demonstrates different opinions from one member to another. Then, there is a disagreement in ranking value for the three risk factors. In case average out of difference is considered, the different combination of three risk factors may produce an identical RPN value for different failure modes. In the present work, the modified RPN prioritization method is introduced into traditional FMEA to solve the above issue and this method is applied in the risk evaluation of water leakage in the building. Finally, the proposed method has been evaluated using statistical analysis techniques. The result indicates that the proposed method is useful for RPN evaluation and prioritization of failure modes.

Keywords: Failure Modes, Risk Factors, Risk Priority Number, Risk Prioritization, Statistical Analysis.

1. INTRODUCTION

Failure Mode and Effects Analysis (FMEA) is a method used for evaluating a product or a process for possible failures. It is used to quantify and record the risk level associated with each potential failure mode for the prioritization and review process. In 1963, FMEA was first used by NASA in the product design phase [1]. FMEA is carried out for each element of a system and sub-system. It determines the effect of failure mode on the system performance. Design and process FMEA were introduced in early period then variants of its kind like system, service, software and maintenance. FMEAs were developed for different applications [2]. FMEA is a popular tool that allows us to prevent a product or a process failure before they occur. It is used to reduce failure cost by identifying early in the product development cycle [3]. FMEA is a proactive tool which is commonly used in Engineering and Medical field. It is widely used in new product design, process and service to identify potential failure modes and determine its effect before they occur [4]. Design FMEA is applied in the design process to avoid design complications and in turn to reduce failure cost. It is further extended to manufacturing phase to improve product quality and reliability [5]. FMEA is a systematic approach to evaluate a product, process and service for improvement. It identifies possible potential failure modes and estimates its severity, occurrence and detection [6].

Sankar and Prabhu introduce a new technique for prioritization of risk using risk priority ranks (RPRs) in a system failure mode and effects analysis. The conventional RPN technique uses a

numeric scale from 1 to 10. It attempts to quantify risk without adequately quantifying the factors that contribute to risk and in some cases the RPN can be misleading the prioritization of risk. It is eliminated by the RPR, the risk is represented using the integers 1 through 1, 000 [7]. Jafari et al. first used the Machinery Failure Mode and Effects Analysis (MFMEA) with risk matrix for the study on reliability of a tunnel boring machine in tunneling [8]. The traditional FMEA process is carried out by the cross functional team, generally the FMEA team has different opinions from one member to another. It is difficult to incorporate the different assessment information in the FMEA process by the RPN model. Piltan et al. present Multi Input Single Output (MISO) fuzzy expert system in the calculation of RPN [9]. Chang et al. present the linguistic ordered weighted geometric averaging (LOWGA) operator in process FMEA [10]. Joo et al. analyze wrinkling and bursting defects of a hydroformed automotive part during flange hydroforming process. In order to increase the reliability of the part, the FMEA approach was used to study the relationship between process parameters and defects [11].

FMEA is a widely used systematic process to identify the possible potential failure modes of a system and process. Many researchers proposed various modified FMEA process including failure cost, fuzzy logic, grey theory, utility priority number, life cost based FMEA and many more. It was found that these approaches do not solve the drawback of traditional FMEA process as mentioned in the problem statement. The main objective of this present study was to introduce a modified risk evaluation and prioritization methodology for design FMEA process. It is a unique and novel approach for prioritization of risk, when the FMEA team has different opinions in ranking scale.

2. FMEA STANDARDS

There are a number of FMEA standards developed and recommended for different applications. Some of important standards are MIL-P-1629, AIAG and SAE J-1739.The FMEA discipline was developed by the United States Military and introduced the military procedure, titled “Procedures for Performing a Failure Mode, Effects and Criticality Analysis MIL-P-1629”, in November 9, 1949.

The objective of the MIL standard is to identify failure modes of critical components of a system with its effect. The International Organization for Standardization (ISO) published the ISO 9000 series of business management standards in the year 1988. The requirements of 1SO-9000 forced organizations to develop formal Quality Management Systems (QMS) that are concentrated on the needs, and expectations of customers. A task force representing Chrysler Corporation, Ford Motor Company, and General Motors Corporation introduced QS-9000 to standardize automotive supplier quality systems. In accordance with QS-9000, automotive suppliers shall use Advanced Product Quality Planning (APQP), which includes design and process FMEAs. The Automotive Industry Action Group (AIAG) and the American Society for Quality Control (ASQC) copyrighted industry-wide FMEA standards in February, 1993. That was the technical equivalent of the Society of Automotive Engineers procedure SAE J-1739. The standards and guidelines are presented in the FMEA Manual are approved and supported by all three automakers [12].

A trial and error method was followed prior to the introduction of FMEA procedure to identify what could go wrong with a product (or) process. Later it was found that it is a time consuming process and steered to wastage of resources in some situation. Otherwise, FMEA is a structured systematic approach used to identify failure modes, its effects and causes. Application of FMEA helps organizations to improve customer satisfaction, safety and comfort.

3. PROCEDURE

Failure Mode and Effects Analysis (FMEA) is accomplished through step-by-step process in the conceptual design phase to identify potential design weaknesses. The objective of FMEA is to identify potential failure modes that may affect safety and product performance [13]. Normally FMEA is carried out by a team of members from design, production, assembly, testing and quality control departments. The team identifies the product failure modes and assigns ranking for

severity, occurrence and detection indexes. The risk level is measured using the Risk Priority Number (RPN). The RPN is a product of the severity, occurrence and detection ranking value. Then, the failure modes are prioritized based on RPN value. The importance will be given to the failure mode which produces higher RPN value.

RPN = Severity ranking (S) x Occurrence ranking (O) x Detection ranking (D) (1)

Severity is ranked based on the effect of failure, Occurrence is the frequency of the failure and Detection is the ability to detect the failure [14]. Figure 1 shows the various steps involved in the FMEA process.

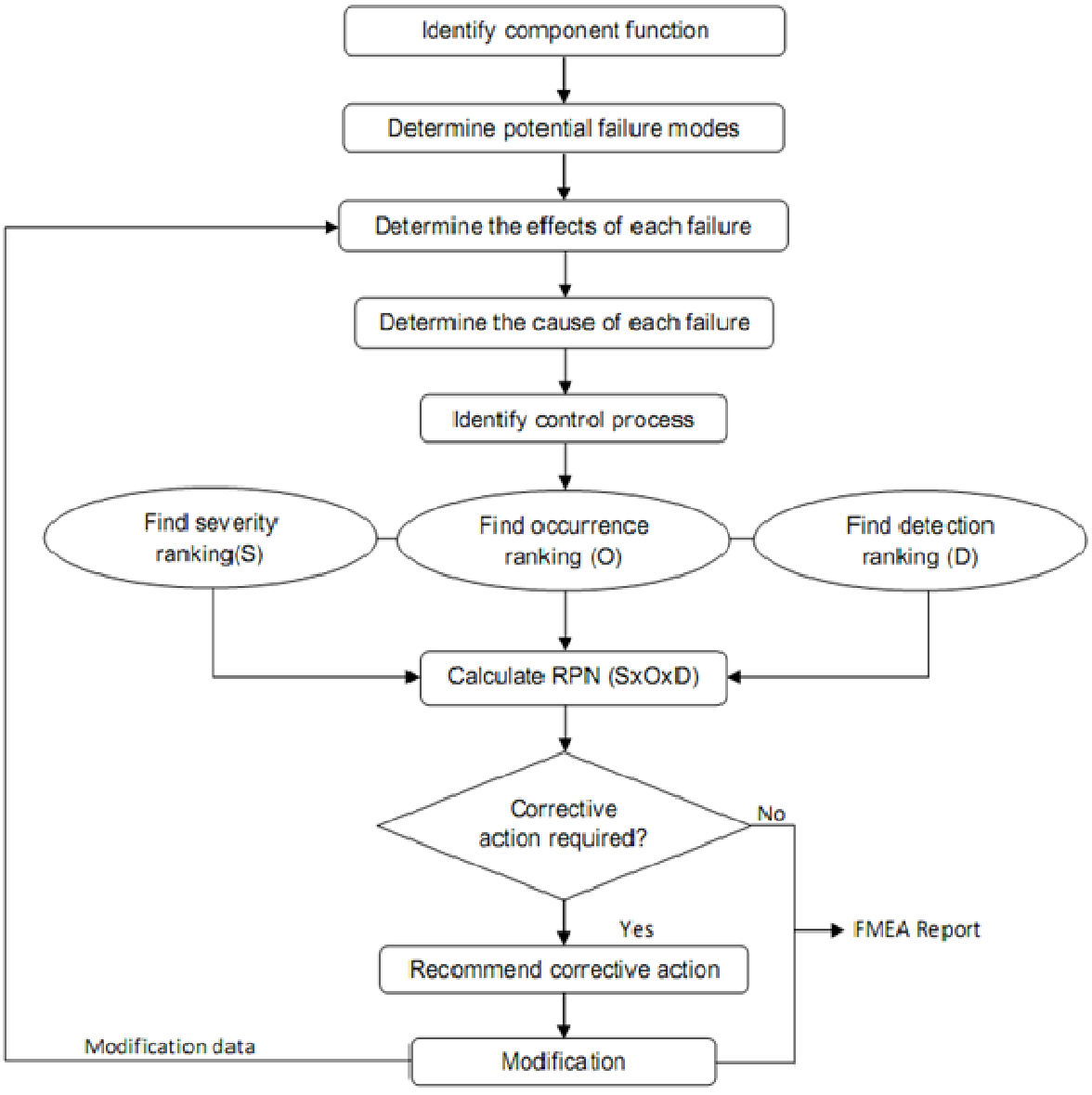

FIGURE 1: FMEA Process.

Table 1 shows the ranking scales (1 – 10) used to measure the severity, occurrence and detection. The calculation of the RPN helps the FMEA team to analyze all the possible failure modes and to identify the most critical failure mode which needs to be addressed immediately.

Accordingly, the FMEA team proposes corrective action to reduce the risk of failure modes. Then, it is re-evaluated after the implementation of corrective action.

Rank	Severity (S)	Occurrence (O)	Detection (D)
10	Hazardous without warning	Extremely high	Absolutely uncertainty
9	Hazardous with warning	Very high	Very remote
8	Very high	High	Remote
7	High	Frequent	Very low
6	Moderate	Moderate	Low
5	Low	Occasion	Moderate
4	Very low	Slight chance	Moderately high
3	Minor	Very slight chance	High
2	Very minor	Remote, very unlikely	Very high
1	None	Extremely remote	Almost certain

TABLE 1: Ranking Scale for Severity, Occurrence and Detection Indexes.

4. PROBLEM STATEMENT

The traditional FMEA approach proposed no threshold value for evaluation of RPNs. There is no value above which it is mandatory to take a recommended action or below which the team is automatically excused from an action. The most critically debated disadvantage of the traditional FMEA is that taking average or higher numerical value for the severity, occurrence and detection indexes, when the FMEA team has a disagreement in the ranking scale. For example, if one member says 6 and someone else says 7, the ranking in this case should be 7 (6+7=13, 13/2=6.5), however this may produce an identical value of RPN.

5. PROPOSED RPN PRIORITIZATION METHODOLOGY

The purpose of the present study is for the development of modified prioritization of risk priority number in design FMEA, when there is a disagreement in ranking scale for severity, occurrence and detection indexes. The modified design FMEA method is used for investigation of water leakage in a building design. The proposed risk prioritization method helps to analyze the possible failure modes and its effects of water leakage in a more systematic approach.

Table 2 shows five common possible failure modes identified for water leakage in buildings. It includes failure modes from rain water leakage, leakage from water installations and drainage leakage in the buildings. The water leakage will have different consequences depending on where it occurs. In rooms with drain system, the water can run out without making damage and the repair cost will be low. It will lead to more extensive damage, if the water leakage is found

where there is no drain system like in living rooms, hall and hidden spaces. In this case, the repair cost also will be high, if it is not stopped immediately.

The RPNs for the possible five failure modes due to water leakage in a building are tabulated in Table 2. It is noticeable that all failure modes are produced an identical value of average RPN. One of the drawbacks in the traditional FMEA is that more than one failure modes will produce an identical value of RPN. Therefore it is suggested that, consider all proposed ranking indexes, if there is a disagreement in the ranking process. Then, calculate RPN range for each failure mode and the failure mode with the lowest RPN range will be evaluated first to establish the control plan to eliminate or to reduce the effect. The risk of each failure is prioritized based on the RPN range, when risk priority number (RPN) average is same for more than one failure modes.

This situation arises when there is a disagreement in the ranking score for the risk factors among the team members. Hence, a general statement is given as **"The higher the RPN mean is more severe. When the RPN means are same, the smaller the RPN range is more severe".**

6. METHODOLOGY

The data presented in the Table 2 was analyzed for the purpose of evaluating the proposed risk evaluation and prioritization method. The proposed method was evaluated using statistical analysis methods like Multiple Regression Analysis, Analysis of Variance (ANOVA), Multi-collinearity Analysis and Residual Analysis with help of SPSS (Statistical Package for the Social Sciences) program.

6.1 Multiple Regression Analysis

Multiple regression is a statistical technique is more suitable method to examine the relationship between a dependent variable and an independent or predictor variables. The independent variables may be quantitative or qualitative and this method helps us to study the effect of one or more variables with other variables [15].

In this research work, we are interested in predicting RPN values (y) using three predictors namely Severity (x1), Occurrence (x2) and Detection (x3).

A multiple regression equation for predicting y can be expressed as follows;

$$y = A + B1\ x1 + B2\ x2 + B3\ x3 \quad (2)$$

Where;

y = Dependent variable RPN
x1, x2, and x3 = Three independent variables S, O and D
B1, B2, and B3 = Co-efficient of the three independent variables
A = Constant

Test hypothesis and null hypothesis are stated as;

$$H0: B1 = B2 = B3 = 0 \quad (3)$$

$$Ha: \text{at least one } Bi \neq 0 \quad (4)$$

(At least one of the coefficients is not zero)

For the regression model to be valid, there are three assumptions to be checked on the residues:

(i) No outliers.
(ii) Independency of data points.
(iii) Residuals are normally distributed with constant variance.

Failure mode	Effect of failure	Cause of failure	Current control	Severity (S)	Occurrence (O)	Detection (D)	RPN[1]	RPN Average	RPN Range	RPN Rank
Leakage in roofing material	Dripping or water flow in the building during and after rain	Aging of material	Use tested material for aging in a climate as on site	3 4	4 5	5	60, 75, 80, 100[1]	78.75	40	1
Leakage from roofing felt joint	Dripping or water flow in the building during and after rain	Poor workman-ship	Have control system for workmanship	5	2 5	3 6	30, 60, 75, 150	78.75	120	3
Leakage from joint to walls	Dripping or water flow in the building during and after rain	Montage error	Rain should not be able to come under the roof material at joint	4 5	3 7	3 4	36, 48, 84, 112, 45, 60, 105, 140	78.75	104	2
Leakage from drains and watertight floors	Dripping or water flows	Montage error, leakage through joints	Look for crack	3 4	5	4 7	60, 105, 80, 140	96.25	80	5
Leakage from pipe fittings	Wall damage	Leakage from joints between pipes	Areas around pipe fittings make watertight solutions	7	2 3	5 6	70, 84, 105, 126	96.25	56	4

TABLE 2: Potential Failure Modes and Prioritization of RPN for Water Leakage Problems in Buildings.

[1]RPN = Risk Priority Number. RPN values are produced by different combinations of S, O and D ranking scales.
For example 3x4x5=60, 3x5x5=75, 4x4x5=80, 4x5x5=100

Model	Unstandardized Coefficients		Standardized Coefficients	t	Sig.	95.0% Confidence Interval for B		Correlations			Collinearity Statistics	
	B	Std. Error	Beta			Lower Bound	Upper Bound	Zero-order	Partial	Part	Tolerance[1]	VIF
1 (Constant)	-134.184	15.975		-8.399	.000	-167.508	-100.860					
Severity	14.039	1.926	.537	7.289	.000	10.021	18.057	.171	.852	.475	**.780**	**1.282**
Occurrence	18.184	1.486	.915	12.236	.000	15.084	21.284	.540	.939	.797	**.759**	**1.318**
Detection	16.575	1.722	.639	9.624	.000	12.983	20.168	.515	.907	.627	**.963**	**1.038**

TABLE 3: Multiple Regression Analysis for RPN.

[1]Tolerance = 1 / VIF (1/1.282 = 0.780, 1/1.318 = 0.759, 1/1.038 = 0.963)

6.2 Analysis of Variance (ANOVA)

The next part of the output contains an analysis of variance (ANOVA) that tests whether the model is significantly better at predicting the RPN. The ANOVA table 4 shows the "usefulness" of the multiple regression model.

Model		Sum of Squares	Degrees of freedom	Mean Square	F	Sig.
1	Regression	23316.590	3	7772.197	71.765	.000a
	Residual	2161.243	20	108.062		
	Total	25477.833	23			

TABLE 4: Analysis of Variance for RPN.

Model	R	R Square	Adjusted R Square	Std. Error of the Estimate	Change Statistics					Durbin-Watson
					R Square Change	F Change	df1	df2	Sig. F Change	
1	.957a	.915	.902	10.395	.915	71.923	3	20	.000	1.807

TABLE 5: Regression Model Summary for RPN.

$$\text{R Square} = \frac{RR_{\text{Regression}}}{RR_{Total}} \tag{5}$$

$$\text{R Square} = \frac{23316.590}{25477.833} = 0.915 \tag{6}$$

$$\text{Test statistic,} \quad F = \frac{R^2 / k}{(1-R^2)/(n-k-1)} \tag{7}$$

Where; $R^2 = 0.915$

k = number of independent variables = 3

n = number of date points = 24

(n-k-1) = degrees of freedom = 24-3-1 = 20

$$F = \frac{.915/3}{(1-.915)/20} = 71.765 \tag{8}$$

6.3 Multi-collinearity Analysis

Often, two or more of the independent variables used in a regression model contribute redundant information. That is, the independent variables are correlated with each other. Table 2 presents data on RPN values for five failure modes with corresponding values of S, O and D for a sample size of 24.

The model is fit to the 24 data points in Table 2 and a portion of the output is shown in Table 3. A formal method of detecting multicollinearity is by means of "Variation Inflation Factors (VIF)". The variation inflation factors measure how much the variances of the estimated regression coefficients are inflated when compared to the predictor variables that are not linearly related.

The general rule of thumb is;

VIF≤1	-	There is no multicollinearity exists among the predictors.
1<VIF≤4	-	May be moderately correlated and can be ignored.
5≤VIF<10	-	Warrant further investigation.
10≤VIF	-	Serious multicollinearity requiring correction.

Multicollinearity exists when tolerance is below .1

$$\text{Tolerance} = 1 - R^2 \quad (9)$$

$$\text{Variation Inflation Factor (VIF)} = 1/\text{Tolerance} \quad (10)$$

7 RESULTS AND DISCUSSION

7.1 Statistical Analysis Results

The statistical analysis is performed using SPSS program. In multiple regression, the model takes the form of an equation that contains a coefficient (B) for each predictor. The first part of the table gives us estimation for these B values and these values indicate the individual contribution of each predictor to the model.

From the output given in Table 3, the regression equation can be written as;

$$y = -134.184 + 14.039*S + 18.184*O + 16.575*D \quad (11)$$

- The B value gives the relationship between RPN and each predictor. If the value is positive, then there is a positive relationship between the outcome and the predictors, whereas a negative coefficient represents a negative relationship.
- From the data shown in the Table 3, all the three predictors have positive B values indicating positive relationship.
- The data points are independent and predictors (severity, occurrence and detection) have positive relationship, hence, the model is valid.
- All of the VIF_k are less than 4 and tolerance is greater than .1 (highlighted in the Table 3), suggesting that there is no multicollinearity is present among the three predictors.

The Analysis of variance (ANOVA) for RPN is presented in Table 4, which shows the sum of squares, mean squares and significance.

- ✓ From Table 4, we see that F = 71.765 and p = 0.000. This is enough to tell us that the p-value or significance of the F is p<.001. Since this is the smallest value at which we can reject the hypothesis, we can reject at .05, .01 and .001.

- ✓ At the α = 0.05 level of significance, there exists enough evidence to conclude that at least one of the predictors is useful for predicting RPN; therefore the model is useful for RPN evaluation and prioritization.

The regression model summary for RPN is presented in Table 5 and the column labeled R is the values of the multiple correlation coefficients between the predictors (severity, occurrence and detection) and the outcome (RPN). The next column gives us a value of R^2, which is a measure of how much of the variability in the outcome is accounted by the predictors.

- The R Square value is 0.915; therefore about 91.5 % of the variation in the RPN is explained by severity, occurrence and detection and hence the model is valid at .95 confidence interval.

- The Durbin-Watson estimate ranges from zero to four. Values distributed around two showed that the data points are independent. Values near zero mean strong positive correlations and four indicates strong negative. In this model the value Durbin Watson is 1.807, which is so close to 2, hence, the independency of data point's assumption is met.

Figure 2 shows that most (95 percent) of the standard residuals are falls within two standard deviations of the mean, which is -2 to +2 and all of them are placed within ±3 standard deviation. More residuals are distributed around zero line and fewer residuals are away from zero.

Figure 3 shows a normal probability plot of the standardized residuals. It shows that the residuals are close to the diagonal line, which means the normality condition is met.

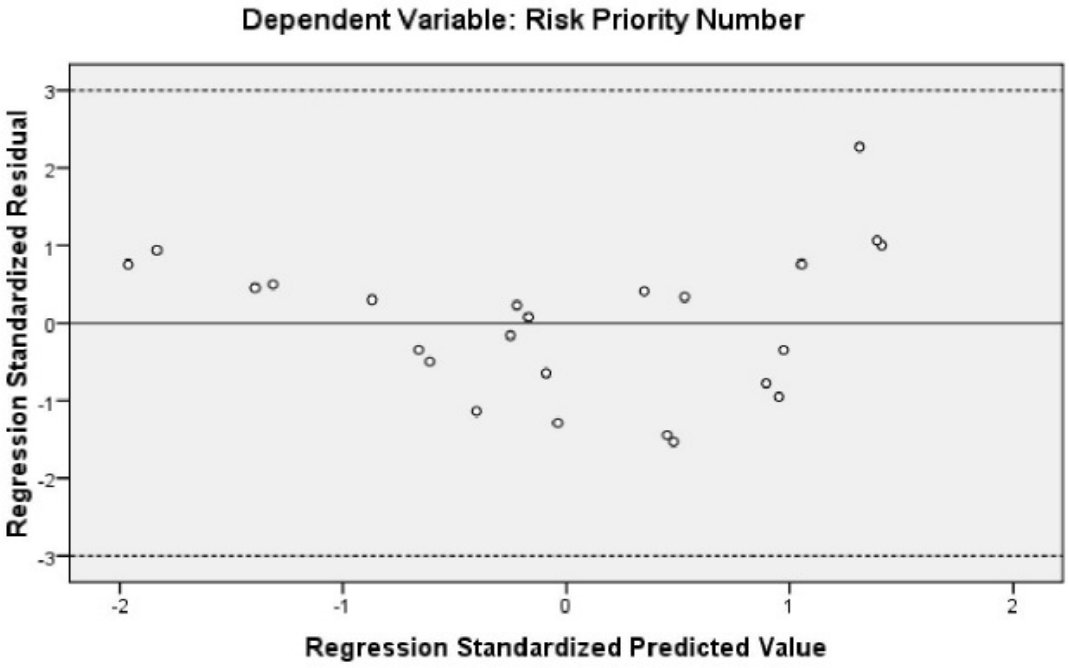

FIGURE 2: Scatter Plot of Standard Residuals.

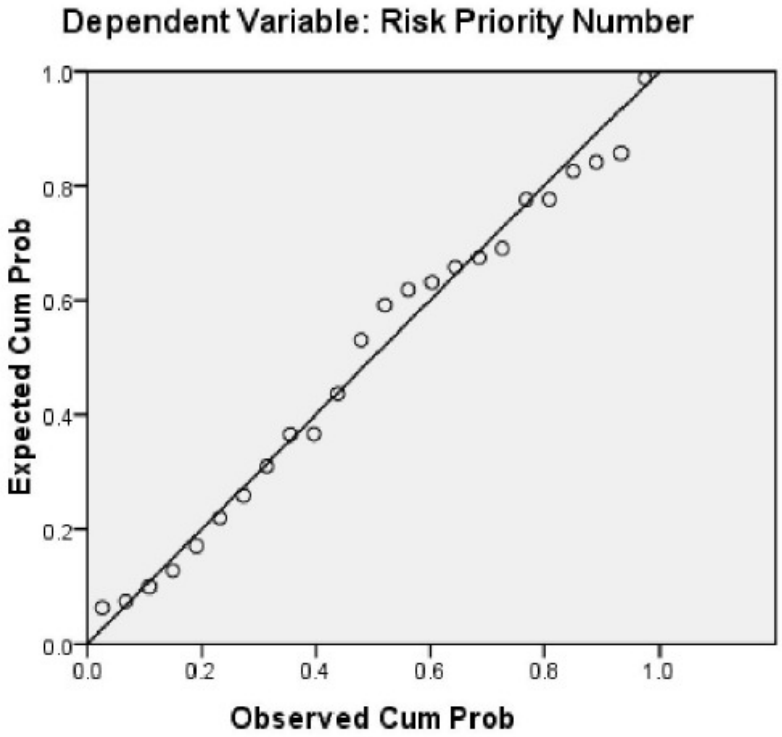

FIGURE 3: Normal Plot of Regression Standardized Residuals.

8. CONCLUSION

The aim of this present paper is to develop an effective modified RPN evaluation and failure mode prioritization method for FMEA to improve the traditional approach. The case study demonstrates that the proposed risk prioritization method is useful in risk evaluation, ranking and prioritization of failure modes;

- When there is a disagreement in ranking score for the three risk factors namely the severity, occurrence and detection.

Finally, the statistical analysis like multiple regression analysis and residual analysis provides a strong evidence for the usefulness of the overall model.

9. REFERENCES

1. Y. Zare Mehrjerdi. “A chance constrained multiple objective goal programming model of fuzzy QFD and FMEA: Model development.” *International Journal of Applied Operational Research*, Vol. 2, pp. 41-53, 2012.

2. C. Jegadheesan, V. P. Arunachalam, S. R. Devadasan and P. S. S. Srinivasan. “Design and development of modified service failure mode and effects analysis model.” International Journal of Services and Operations Management, Vol. 3, pp. 111-126, 2007.

3. Khalid S. Mekki. “Robust design failure mode and effects analysis in designing for six sigma.” International Journal of Product Development, Vol. 3, pp. 292-304, 2006.

4. J. W. Senders. “FMEA and RCA: The mantras of modern risk management.” Journal of Quality and Safety in Health Care, Vol. 13, pp. 249-250, 2004.

5. Sheng-Hsien Teng, and Shin-Yann Ho. “Failure mode and effects analysis an integrated approach for product design and process control.” International Journal of Quality & Reliability Management, Vol. 13, pp. 8-26, 1996.

6. Suhendra Werner, Witt Fred and Compart. “Assessing Safety in Distillation Column using Dynamic Simulation and Failure Mode and Effect Analysis (FMEA).” Journal of Applied Sciences, Vol. 7, pp. 2033-2039, 2007.

7. N. R. Sankar and B. S. Prabhu. “Modified approach for prioritization of failures in a system failure mode and effects analysis.” International Journal of Quality & Reliability Management, Vol. 18, pp. 324-335, 2000.

8. M. J. Jafari, N. Gharari and H. R. Sheikhi. “The Reliability of a Tunnel Boring Machine.” International Journal of Occupational Hygiene, Vol. 1, pp. 20-25, 2009.

9. M. Piltan, R. Ghodsi, F. Quarashi and M. Azizian. “Analysis of Potential Failure Modes in an Assembly Line by Fuzzy Expert Systems. Journal of Mechanics Engineering and Automation, Vol. 1, pp. 445-449, 2011.

10. K. Chang, Y. Chang, T. Wen and C. Cheng. “An innovative Approach Integrating 2-Tuple and LOWGA Operators in Process Failure Mode and Effects Analysis.” International Journal of Innovative, Computing, Information and Control, Vol. 8, pp. 747-761, 2012.

11. B. Joo, S. Kim and Y. H. Moon. “FMEA for the reliability of hydroformed flanged part for automotive application.” Journal of Mechanical Science and Technology, Vol. 27, pp. 63-67, 2013.

12. K. A. Lange, S. C. Leggett and B. Baker. “Potential Failure Mode and Effects Analysis (FMEA) Reference Manual.” 3rd Ed. Daimler Chrysler, Ford, General Motors, USA, 2001.

13. B. Almannai, R. Greenough and J. Kay. “A decision support tool based on QFD and FMEA for the selection of manufacturing automation technologies.” Robotics and Computer-Integrated Manufacturing, Vol. 24, pp. 501-507, 2008.

14. Kai Meng Tay and Chee Peng Lim. “Fuzzy FMEA with a guided rules reduction system for prioritization of failure.” International Journal of Quality & Reliability Management, Vol. 23, pp. 1047-1066, 2006.

15. Dale E. Berger. “Introduction to Multiple Regression.” Claremont Graduate University, USA. Available: wise.cgu.edu/downloads/Regression.doc [2003].

INSTRUCTIONS TO CONTRIBUTORS

The *International Journal of Engineering (IJE)* is devoted in assimilating publications that document development and research results within the broad spectrum of subfields in the engineering sciences. The journal intends to disseminate knowledge in the various disciplines of the engineering field from theoretical, practical and analytical research to physical implications and theoretical or quantitative discussion intended for both academic and industrial progress.

Our intended audiences comprises of scientists, researchers, mathematicians, practicing engineers, among others working in Engineering and welcome them to exchange and share their expertise in their particular disciplines. We also encourage articles, interdisciplinary in nature. The realm of International Journal of Engineering (IJE) extends, but not limited, to the following:

To build its International reputation, we are disseminating the publication information through Google Books, Google Scholar, Directory of Open Access Journals (DOAJ), Open J Gate, ScientificCommons, Docstoc and many more. Our International Editors are working on establishing ISI listing and a good impact factor for IJE.

The initial efforts helped to shape the editorial policy and to sharpen the focus of the journal. Started with volume 7, 2013, IJE appears with more focused issues. Besides normal publications, IJE intend to organized special issues on more focused topics. Each special issue will have a designated editor (editors) – either member of the editorial board or another recognized specialist in the respective field.

We are open to contributions, proposals for any topic as well as for editors and reviewers. We understand that it is through the effort of volunteers that CSC Journals continues to grow and flourish.

IJE LIST OF TOPICS

The realm of International Journal of Engineering (IJE) extends, but not limited, to the following:

- Aerospace Engineering
- Agricultural Engineering
- Biomedical Engineering
- Chemical Engineering
- Civil & Structural Engineering
- Computer Engineering
- Control Systems Engineering
- Education Engineering
- Electrical Engineering
- Electronic Engineering
- Engineering Mathematics
- Engineering Science
- Environmental Engineering
- Fluid Engineering
- Geotechnical Engineering
- Industrial Engineering
- Manufacturing Engineering
- Materials & Technology Engineering
- Mechanical Engineering
- Mineral & Mining Engineering
- Nuclear Engineering
- Optical Engineering
- Petroleum Engineering
- Robotics & Automation Engineering
- Telecommunications Engineering

CALL FOR PAPERS

Volume: 7 - **Issue:** 2

i. Paper Submission: April 30, 2013 **ii. Author Notification:** May 31, 2013

iii. Issue Publication: June 2013

CONTACT INFORMATION

Computer Science Journals Sdn BhD
B-5-8 Plaza Mont Kiara, Mont Kiara
50480, Kuala Lumpur, MALAYSIA

Phone: 006 03 6207 1607
006 03 2782 6991

Fax: 006 03 6207 1697

Email: cscpress@cscjournals.org

CSC PUBLISHERS © 2013
COMPUTER SCIENCE JOURNALS SDN BHD
M-3-19, PLAZA DAMAS
SRI HARTAMAS
50480, KUALA LUMPUR
MALAYSIA

PHONE: 006 03 6207 1607
FAX: 006 03 6207 1697
EMAIL: cscpress@cscjournals.org